

RESEARCH PAPER



## Reutericyclin, a specialized metabolite of *Limosilactobacillus reuteri*, mitigates risperidone-induced weight gain in mice

Fatima A. Aboulazm<sup>a\*</sup>, Alexis B. Kazen<sup>a\*</sup>, Orlando deLeon<sup>a\*</sup>, Susanne Müller<sup>a</sup>, Fatima L. Saravia<sup>a</sup>, Valery Lozada-Fernandez<sup>a</sup>, Matthew A. Hadiono<sup>a</sup>, Robert F. Keyes<sup>b,c</sup>, Brian C. Smith<sup>b,c</sup>, Stephanie L. Kellogg<sup>a</sup>, Justin L. Grobe<sup>d,e,f,g</sup>, Tammy L. Kindel<sup>h,i</sup>, and John R. Kirby<sup>a,g,i</sup>

<sup>a</sup>Department of Microbiology & Immunology, Medical College of Wisconsin, Milwaukee, WI, USA; <sup>b</sup>Department of Biochemistry, Medical College of Wisconsin, Milwaukee, WI, USA; <sup>c</sup>Program in Chemical Biology, Medical College of Wisconsin, Milwaukee, WI, USA; <sup>d</sup>Department of Physiology, Medical College of Wisconsin, Milwaukee, WI, USA; <sup>e</sup>Department of Biomedical Engineering, Medical College of Wisconsin, Milwaukee, WI, USA; <sup>f</sup>Comprehensive Rodent Metabolic Phenotyping Core, Medical College of Wisconsin, Milwaukee, WI, USA; <sup>g</sup>Cardiovascular Center, Medical College of Wisconsin, Milwaukee, WI, USA; <sup>h</sup>Department of Surgery, Medical College of Wisconsin, Milwaukee, WI, USA; <sup>i</sup>Center for Microbiome Research, Medical College of Wisconsin, Milwaukee, WI, USA

### ABSTRACT

The role of xenobiotic disruption of microbiota, corresponding dysbiosis, and potential links to host metabolic diseases are of critical importance. In this study, we used a widely prescribed antipsychotic drug, risperidone, known to influence weight gain in humans, to induce weight gain in C57BL/6J female mice. We hypothesized that microbes essential for maintaining gut homeostasis and energy balance would be depleted following treatment with risperidone, leading to enhanced weight gain relative to controls. Thus, we performed metagenomic analyses on stool samples to identify microbes that were excluded in risperidone-treated animals but remained present in controls. We identified multiple taxa including *Limosilactobacillus reuteri* as a candidate for further study. Oral supplementation with *L. reuteri* protected against risperidone-induced weight gain (RIWG) and was dependent on cellular production of a specialized metabolite, reutericyclin. Further, synthetic reutericyclin was sufficient to mitigate RIWG. Both synthetic reutericyclin and *L. reuteri* restored energy balance in the presence of risperidone to mitigate excess weight gain and induce shifts in the microbiome associated with leanness. In total, our results identify reutericyclin production by *L. reuteri* as a potential probiotic to restore energy balance induced by risperidone and to promote leanness.

### ARTICLE HISTORY

Received 26 April 2024  
Revised 14 January 2025  
Accepted 5 March 2025

### KEYWORDS

Risperidone; reutericyclin; anti-obesogenic; energy balance; *Limosilactobacillus reuteri*; random forest; ridge regression; specialized metabolites; shotgun metagenomics

## Introduction

Gut microbes have the capacity to produce a vast reservoir of specialized metabolites<sup>1,2</sup> that affect interspecies interactions and ultimately have effects on human health. Bioinformatic analyses of bio-synthetic gene clusters has led to a greater appreciation of the diversity and function of specialized metabolites.<sup>3–5</sup> Specialized metabolites include molecules that act as antibiotics, anticancer therapeutics, and other natural products of interest to the broader healthcare system. Many specialized metabolites are known to affect microbial communities within soil ecosystems where they have been characterized more fully *in vitro*.<sup>6–10</sup>

Xenobiotics, such as psychotropic medications (e.g. fluoxetine), affect responses to specialized metabolites

impacting host health by complex mechanisms that involve gut bacteria.<sup>11</sup> Risperidone is a commonly prescribed second-generation antipsychotic that exacerbates obesity, diabetes, and other negative sequelae in humans.<sup>12</sup> Previously, we demonstrated that risperidone alters the gut microbiome to mediate excessive weight gain leading to obesity in both humans and mice.<sup>13,14</sup> A fecal material transplant of risperidone-altered microbiota was sufficient to suppress the metabolic rate of naive C57BL/6J female mice relative to vehicle controls. Those results suggest that gut microbiota play a causal role during risperidone-induced weight gain (RIWG) by altering energy efficiency. We hypothesize that specific bacterial taxa, otherwise displaced by treatment with risperidone, might protect mice from RIWG.

**CONTACT** John R. Kirby ✉ [jkirby@mcw.edu](mailto:jkirby@mcw.edu) Department of Microbiology & Immunology, Medical College of Wisconsin, 8701 Watertown Plank Road, Milwaukee, 53226 WI, USA

\*Authors contributed equally to this work.

Supplemental data for this article can be accessed online at <https://doi.org/10.1080/19490976.2025.2477819>

© 2025 The Author(s). Published with license by Taylor & Francis Group, LLC.

This is an Open Access article distributed under the terms of the Creative Commons Attribution-NonCommercial License (<http://creativecommons.org/licenses/by-nc/4.0/>), which permits unrestricted non-commercial use, distribution, and reproduction in any medium, provided the original work is properly cited. The terms on which this article has been published allow the posting of the Accepted Manuscript in a repository by the author(s) or with their consent.

To identify bacterial species or strains that might promote leanness, we performed shotgun metagenomic sequencing on stool samples to identify microbes that were excluded in risperidone-treated animals but remain present in relatively lean, untreated controls. We identified several taxa including *Limosilactobacillus reuteri*, known for its production of specialized metabolites,<sup>15</sup> presence in the global food supply,<sup>16</sup> and its ability to be grown and genetically manipulated *in vitro*.<sup>17</sup> We supplemented mice with *L. reuteri* and found that the organism was sufficient to mitigate enhanced weight gain following risperidone treatment. Further, we found that production of the *L. reuteri* specialized metabolite, reutericyclin (Rtc), was necessary to protect mice from RIWG. *L. reuteri*  $\Delta$ rtcN cells, lacking a key component of the reutericyclin biosynthetic gene cluster, were unable to protect mice from RIWG. Lastly, synthetic reutericyclin was able to protect mice from RIWG. Both synthetic reutericyclin and *L. reuteri* were found to restore energy efficiency without altering food consumption or digestive efficiency that could affect RIWG. Together, the data indicate that reutericyclin-producing *L. reuteri* restores energy balance and alters the gut microbiota associated with risperidone treatment.

Additional analyses by machine learning yielded a set of taxonomic features that were sufficient to classify distinct microbiota based on treatment group. Those features were utilized to generate a linear model (ridge regression) capable of predicting weight gain in mice for either synthetic reutericyclin or *L. reuteri* treatment. Although all treatment groups showed increases in Firmicutes (Bacillota) generally, strain-specific pathway analysis from metagenomic data revealed that taxa associated with leanness had enhanced fermentation capacity. Overall, the results support a conclusion that reutericyclin elicits its anti-obesogenic effects by enhancing metabolic capacity by bacteria and preventing caloric uptake by the host. More broadly, strain-specific specialized metabolites may have a primary role as probiotics to prevent unwanted weight gain during treatment with xenobiotics.

## Materials and methods

### Bacterial cultures and growth

*L. reuteri* strains were grown in De Man, Rogosa and Sharpe (MRS) biphasic slants for 16 h overnight at 37°C to stationary phase as previously described.<sup>18</sup> Cultures were then combined and pelleted by centrifugation at 3000xg for 15 min, washed 3X with PBS +Ca/+Mg. The remaining pellet was resuspended in PBS+Ca/+Mg to a concentration of  $3 \times 10^9$ /mL daily prior to gavage. Colony forming units (CFUs) were quantified by serially diluting cultures onto MRS agar plates and grown 16 h under anaerobic conditions using the GasPak system (BD#261201).

### Construction of the $\Delta$ rtcN mutant

The upstream and downstream regions of the *rtcN* gene were amplified using primers rtcNPP1 (AAAGGATCCCCATTAAGATACGATAAAAAGGATTTATC), rtcNPP2 (TTAATGCTCCTTTT TATTTGTTATATTATTAATAAACTTTTGTA-AACTAGTAAGATTCATTGATAACAT) and rctNPP3 (TTTATTAATAATATAACAAAT AAAAAGGAGCATTA), rctNPP4 (AAACTGC AGTTCTATATAATCAACTTGTTCAGGAATGA) with *L. reuteri* LTH2584 chromosomal DNA as template. PCR sewing technology was used to generate a DNA fragment that contained both, the up- and downstream region. The fragment was digested with restriction enzyme PstI and cloned into the temperature sensitive cloning vector pJRS233 resulting in plasmid JK5079. In general *L. reuteri* was grown on MRS slant agar at 37°C. Plasmid JK5079 was electroporated (2500 V, 25  $\mu$ F and 400 Ohm) into competent *L. reuteri* cells that were resuspended in water with 0.5 M sucrose and 10% glycerol. After transformation, the cells were incubated in prewarmed MRS medium and recovered for 1 h at 37°C. MRS medium containing 10  $\mu$ g/ml erythromycin was added to the cells and transferred onto MRS slant agar with 10  $\mu$ g/ml erythromycin. Incubated for 80 generations at 42–44°C followed to select for single crossover mutants. Plasmid integration was verified using primers specific to the erythromycin gene (Ermf CTTATTAAATAATTTATAG CTATTGAA, Ermr CGATAATTTCCAAGTT

TTA). *L. reuteri* with JK5079 integrated into the chromosome were cultured in MRS broth at 37°C for 100 generations to cure the cells of the plasmid. Erythromycin-sensitive double crossover mutants were selected on MRS Agar. The deletion of the *rtcN* gene was verified using primers *rtcN* fwdcheck GATACCGAGAAATAAGTCCA CGT and *rtcN* revcheck CTTCCATGG CATTATAACAGCATT. With these primers an amplicon of 3454 bp was detected with wild type *L. reuteri* and a 454 bp amplicon with the  $\Delta$ *rtcN* mutant strain.

### Animal husbandry and gavage

C57BL/6J female mice (Jackson Laboratories) at six weeks of age were individually housed, provided with Inotiv Teklad 2920X chow, and placed on sterile, acidified water upon arrival and allowed two weeks to acclimate to the animal facility. At eight weeks of age, mice were weight matched and assigned to experimental cohorts. Risperidone was provided *ad libitum* at a concentration of 20 µg/mL and changed twice per week in the drinking water. Administration of reutericyclin (2.5 µg, 100 µL gavage PBS +Ca +Mg, 3% DMSO), *L. reuteri* ( $3 \times 10^8$  CFUs/100 µL of PBS+/+) or vehicle control was administered daily by oral gavage. Fresh stool was collected twice weekly, flash frozen with liquid nitrogen, and stored at -80°C until DNA extraction. Mice were placed in metabolic cages to determine metabolic flux at 7 weeks of age, 9 weeks of age, and 17 weeks of age.

### DNA isolation and library preparation

DNA was isolated from 0.3 g of stool using the PowerSoil DNA Extraction Kit (Qiagen#12888-100). DNA quality was assessed using a NanoDrop spectrophotometer and QuBit (dsDNA HS kit#Q32854). Libraries were prepared using the Illumina TruSeq DNA library prep system. 16S V3-V4 (341-806) libraries were sequenced on an Illumina MiSeq at 2 × 250 paired-end (PE) reads. Shotgun libraries were sequenced on an Illumina HiSeq or an Illumina NovaSeq at 2 × 150PE reads with >10 million reads per sample.

### Sequence analysis

Shotgun raw sequences were quality filtered using Trimmomaticv0.39<sup>19</sup> (Phred33) and Illumina Utils<sup>20</sup> v2.11. Samples were then co-assembled using MegaHit<sup>21,22</sup> v1.2.9 to generate contigs of a minimal length = 1000 bp. Short reads were then mapped back to these contigs using Bowtie<sup>23</sup> v2.5.0 and converted into sorted BAMs using Samtools<sup>24</sup> v1.20. An analysis and visualization platform for 'omics data (Anvi'o)<sup>25,26</sup> was used to visualize and analyze these data. Contigs were imported into Anvi'o v8.0.0 with a minimum length cutoff of 2500 bp and binned into preliminary metagenome assembled genomes (MAGs) using MetaBAT2.<sup>27</sup> Single copy genes defined by Campbell et al. (2013)<sup>28</sup> were used to estimate completion and redundancy for the preliminary MAGs. MAGs were manually curated and considered high quality if completion was >50% and they were >2 Mb in length, or if they had a completion of >90%, and they were considered medium quality if completion was between 50% and 90% but length was <2 Mb. MAGs with <50% completion were considered low quality. All MAGs were refined to have <10% redundancy. Taxonomic identification was achieved using KAIJU.<sup>29</sup> Orthologous protein group IDS from the Kyoto Encyclopedia of Genes and Genomes (KEGG) were used for the functional analysis of the microbiomes. LEfSe<sup>30</sup> was used to identify differentially abundant MAGs with LDA scores >2.0 and  $p < 0.05$ . NCBI BLAST<sup>31</sup> was used to attain species-level resolution of the Lactobacillaceae MAGs.

16S rRNA gene sequencing data was analyzed on the QIIME2 platform<sup>32</sup> v2024.10 and taxonomic classification was obtained using the SILVA v138 reference database. Statistical comparisons of differentially abundance taxa were performed using LEfSe. Random Forest analysis (implemented in R using the 'Boruta' and 'randomForest' packages)<sup>33</sup> was performed on discriminant features to generate Gini coefficients that illustrate the importance of each feature to distinguish between treatment groups. Graphs were generated in PrismGraphpad, SigmaPlot, and 'ggplot2' R package.<sup>34</sup> All statistical analyses in R were performed using R (v4.4.2).

### Metabolic caging & bomb calorimetry

Metabolic phenotyping was conducted as previously described.<sup>35</sup> Briefly, mice were individually housed in metabolic cages (Nalgene) to monitor fluid and food intake daily. Additionally, urine and fecal outputs were measured and collected. Fecal material was utilized to determine digestive efficiency by bomb calorimetry. Caloric densities of desiccated food and fecal samples were determined using a 50 mg semi-micro bomb calorimeter (Parr). Energy absorption was calculated as:

$$\{\text{Energy Absorbed}\} = \{\text{Energy Consumed}\} - \{\text{Fecal Energy}\}$$

Energy Consumed is the product of the dry mass of food consumed and the caloric density of dry food, and Fecal Energy is the product of the dry mass of feces produced and the caloric density of the dried feces. Digestive efficiency was then calculated as:

$$\{\text{Digestive Efficiency}\} = \{\text{Energy Absorbed}\} / \{\text{Energy Consumed}\}$$

Energy efficiency was calculated at various time points after the initiation of risperidone as:

$$\{\text{Energy Efficiency}\} = \{\Delta\text{Body Mass}\} / \{\text{Total Energy Absorbed}\}$$

### Ridge regression analyses for predicting weight gain

Ridge regression model was used to address issue of multicollinearity among predictor variables: selected metagenomes from Boruta and weight gained by mice at end of respective study. Regularization parameters (best lambda) of 0.297088 and 23.82712 were selected after 10-fold cross-validation for LTH2584 and Reutericyclin study, respectively. Model performance was evaluated using Root Mean Squared Error (RMSE) and coefficients were extracted using 'glmnet' package in R.<sup>36,37</sup>

### Scheme for synthesis of reutericyclin is available as a supplementary method

### Results

#### Shotgun metagenomics reveals Lactobacillaceae strains are excluded from the gut following treatment with risperidone

Previously we demonstrated that risperidone excludes specific taxa from the gut using 16S

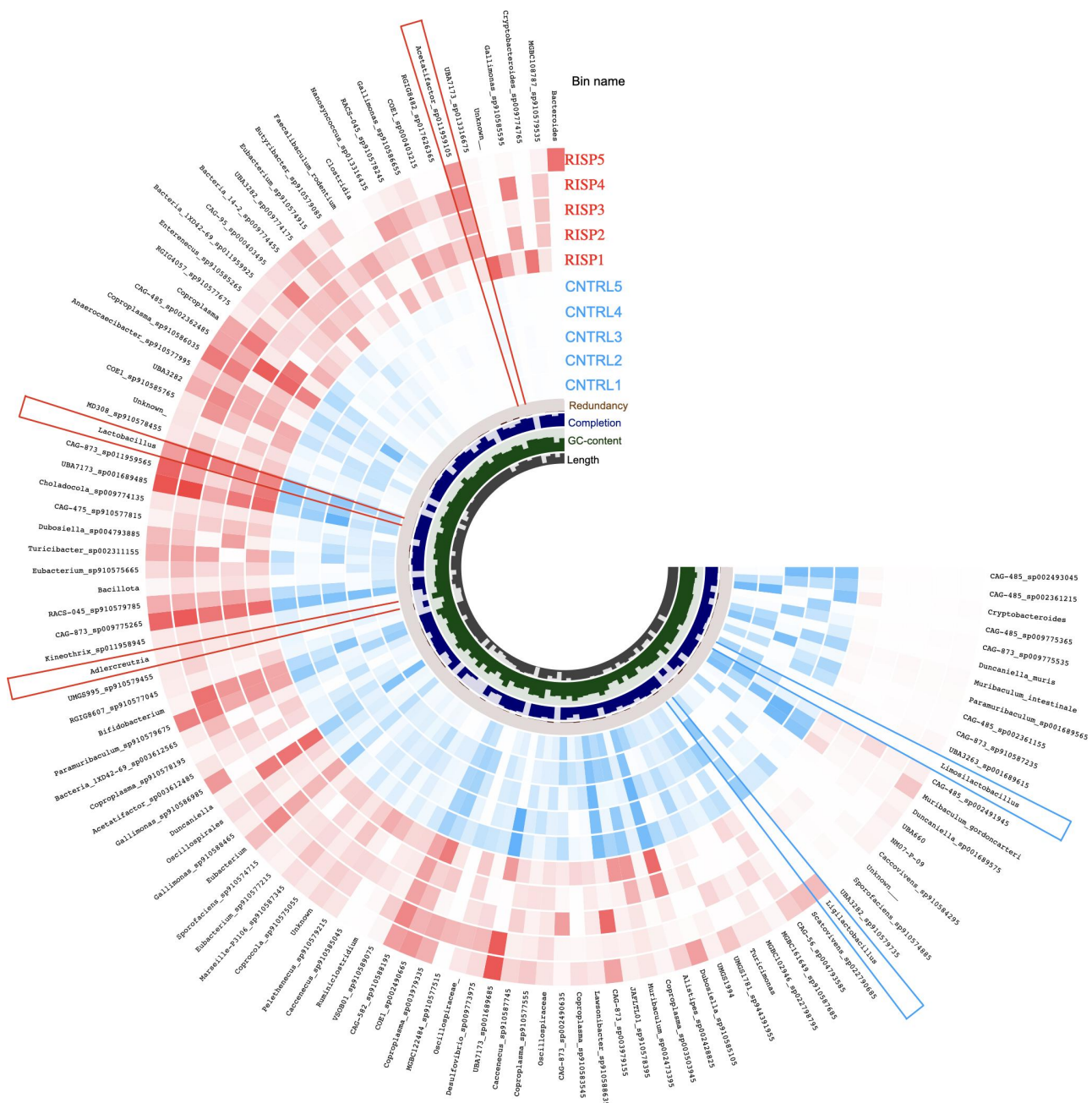
rDNA sequencing.<sup>14</sup> We hypothesized that these bacteria may be important in preventing weight gain during risperidone treatment. 16S sequencing of stool-derived bacterial DNA is typically limited to fragments such as the V3-V4 region of the rDNA gene and is frequently unable to resolve species or strain-level differences within microbiomes. Therefore, we used Illumina-based shotgun metagenomic sequencing to gain resolution of the composition of gut microbiota in risperidone treated C57BL/6J female mice ( $n = 5$ ) and non-treated controls ( $n = 5$ ).

We assembled and binned the bacterial genomes for each mouse and visualized the data using the Anvi'o suite (Figure 1(a))<sup>25,26</sup> as described in Methods. The resulting phylogram depicts microbiomes for each mouse as a concentric ring (red = risperidone-treated animals, blue = control animals), each metagenome as a radial slice, and the abundance of each metagenome is plotted as a function of intensity. The genomes are ordered based on the fold difference in mean coverage for risperidone-treated mice compared to controls.

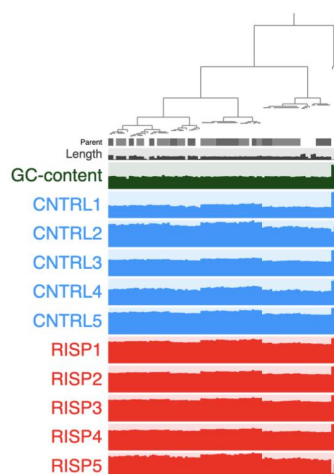
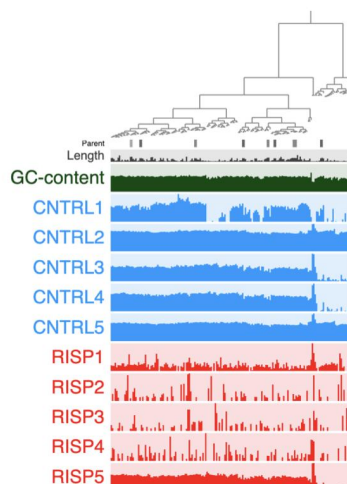
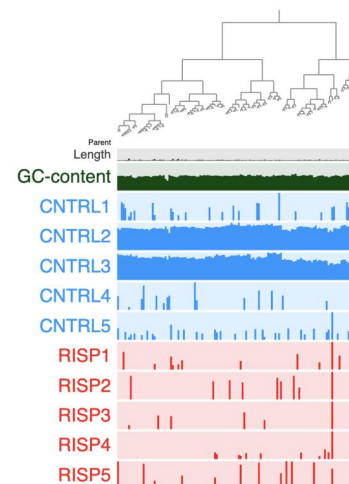
The results are consistent with our previous findings using 16S rDNA sequencing<sup>14</sup> where we found that the microbiota of risperidone-treated animals was either enriched or depleted for specific bacterial taxa relative to controls. We binned a total of 112 genomes with redundancies <10%, where redundancy is defined as the number of genes in a bin occurring more than once but typically found as a single copy in most bacterial genomes (i.e. single copy core genes (SCGs)). Full taxonomic assignments, average abundances in each treatment group, length of each reconstructed metagenome, and binning statistics are included in Supplemental Tables. Binned genomes were subdivided into high quality (>90% completion OR >2Mb and >50% completion; Table S1), medium quality (50–90% completion; Table S2), or low quality (<50% completion; Table S3). The abundances of 16 of the 112 bacterial metagenomes were statistically enriched in controls relative to risperidone-treated animals (Kruskal-Wallis,  $p < 0.05$ ) and all 16 metagenomes have an LDA score >2.0 (Table S4).

Three genomes were resolved at the species level including *Ligilactobacillus murinus*, *Limosilactobacillus reuteri*, and *Lactobacillus*

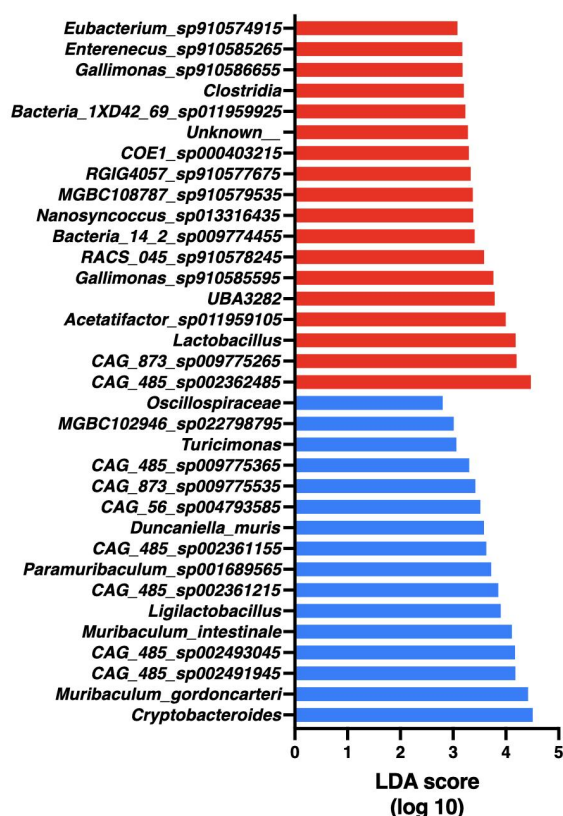




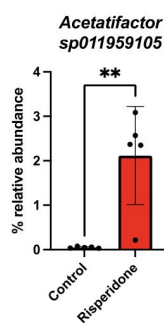
**Figure 1.** Shotgun metagenomics reveals altered gut microbiota following treatment with risperidone. A) Shotgun metagenomics sequencing of stool from C57BL/6J female mice treated with with risperidone ( $n=5$ , 20  $\mu\text{g/mL}$  risperidone, *ad libitum*) was compared to controls ( $n=5$ ) after 60 days of treatment. Circle phylogram represents 112 metagenome assembled genomes (MAGs) organized based on the mean difference in read coverage comparing control and risperidone-treated mice. Each ring represents a single read. Read coverage for each MAG is represented by color intensity (either red or blue, depending on treatment group). Red boxes highlight a subset of metagenomes (*Acetatifactor*, *Adlercreutzia* sp., and *Lactobacillus johnsonii*) that are enriched following treatment with risperidone. *Acetatifactor* and *Adlercreutzia* sp are highlighted due to their role as key features predicting weight change as shown in Figure 10. Blue boxes highlight Lactobacillaceae MAGs (*Ligilactobacillus murinus* and *Limosilactobacillus reuteri*) that are depleted following risperidone treatment. The center of the wheel depicts metagenome completion and redundancy, as determined by using bacterial single-copy genes defined by Campbell *et al.* (2013). Taller bars indicate higher completion or redundancy. % GC content and length for each MAG are displayed at the center of the wheel and are also represented by the height of the bar. MAGs with length bars that reach the top of the panel are at least 2 Mb. B-D) Genome coverage for Lactobacillaceae MAGs (*L. johnsonii*, *L. murinus*, and *L. reuteri*). E) Top discriminatory features as determined by LEfSe. Red MAGs are enriched in risperidone-treated mice, and blue MAGs are enriched in controls. F-J) Relative abundances for *Acetatifactor* sp011959105, *Adlercreutzia*, *L. johnsonii*, *L. murinus*, and *L. reuteri* following treatment with risperidone. \*:  $p < 0.05$ ; \*\*:  $p < 0.01$  via Mann-Whitney U test.

b. *Lactobacillus johnsonii*c. *Ligilactobacillus murinus*d. *Limosilactobacillus reuteri*

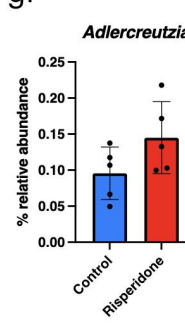
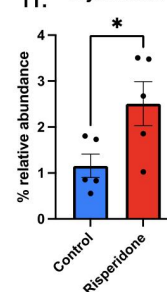
## e. Top discriminatory features (LEfSe)



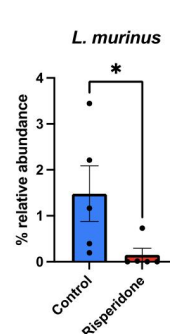
## f.



## g.

h. *L. johnsonii*

## i.



## j.

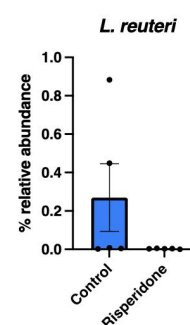
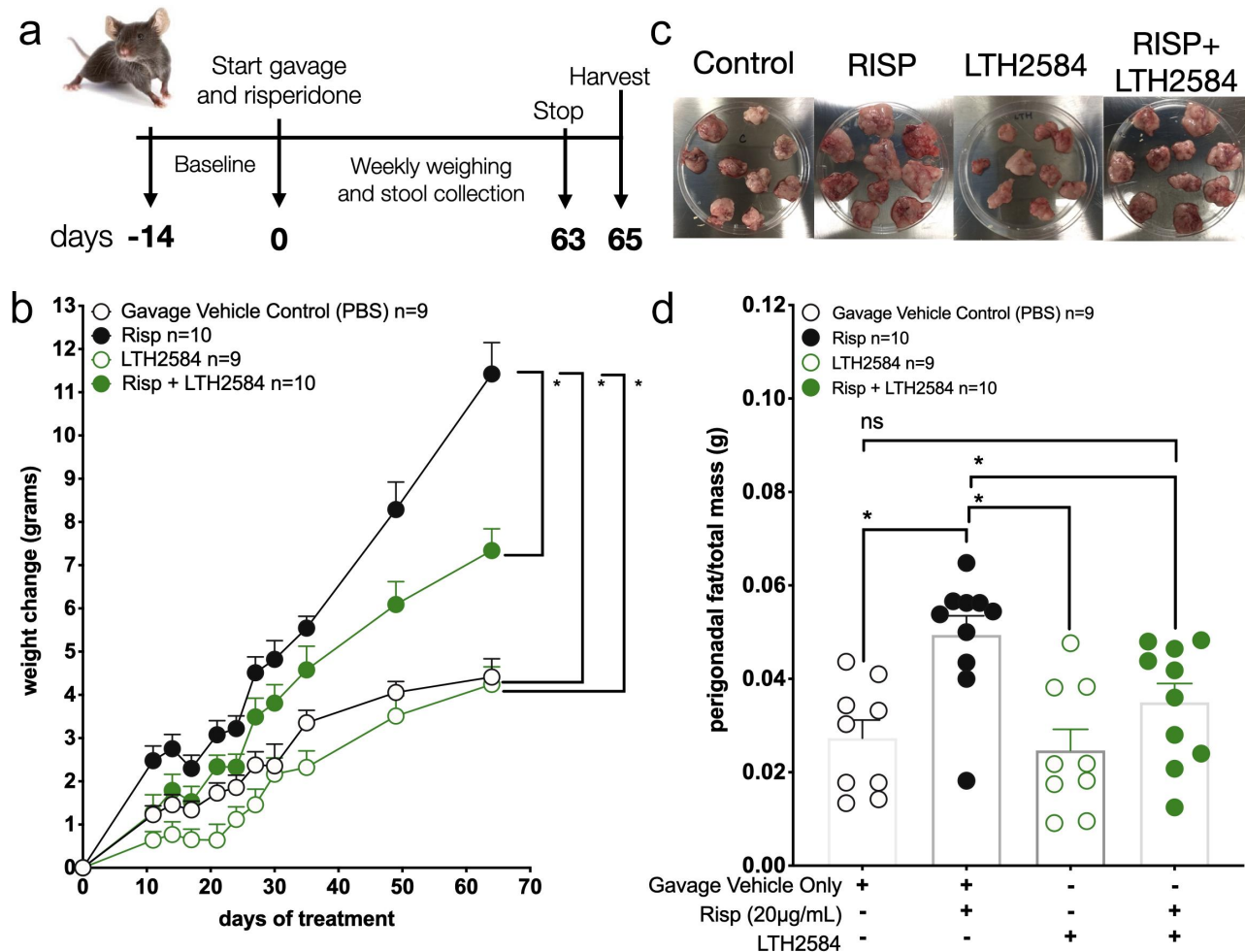


Figure 1. (Continued).

*johnsonii*. The reconstructed *L. murinus* metagenome is 1.7 Mb, the *L. reuteri* metagenome is 0.5 Mb (Figures 1(g,h)), and the *L. johnsonii* metagenome is 1.8 Mb. We found that two of the three Lactobacillaceae metagenomes were present in

control animals but largely depleted in risperidone-treated animals; however, the third Lactobacillaceae metagenome, *Lactobacillus johnsonii*, was enriched in risperidone-treated animals instead.



**Figure 2.** Supplementation with reutericyclin producing *L. reuteri* strain LTH2584 mitigates weight gain during risperidone treatment. A) To test whether supplementation with a reutericyclin-producing *L. reuteri* can mitigate weight gain, we provided *L. reuteri* strain LTH2584 at  $3 \times 10^8$  CFUs/day (100  $\mu$ L PBS) or vehicle control by gavage to C57bl/6J females at 56 days of age (8 weeks) and measured body mass gains over the course of 65 days. Risperidone was provided *ad libitum* (20  $\mu$ g/mL) in the drinking water. B) Weight gain over time. After 9 weeks of treatment, LTH2584-only treated mice (n=10, green open) and gavage vehicle controls (n=10, black open) gained significantly less weight than the risperidone-only treated mice (n=10, black filled) (2-way ANOVA,  $p < 0.001$ ). LTH2584+risperidone-treated animals (n=10, green filled) gained significantly less weight than risperidone-only treated animals (2-way ANOVA,  $p < 0.001$ ), suggesting that *L. reuteri* strain LTH2584 mitigated risperidone-mediated weight gain. C and D) Quantification of the dissected perigonadal fat masses of each mouse demonstrated reduced fat mass in the LTH2584+risperidone treatment group relative to risperidone-only group. The perigonadal fat mass to total mass was then calculated. Risperidone-treated animals had a significantly higher ratio compared to all other treatment groups (Pairwise Mann-Whitney,  $p < 0.01$ ), while Risperidone+LTH2584 treated animals were not statistically different from vehicle controls or LTH2584 alone (Pairwise Mann-Whitney,  $p > 0.05$ ).

#### Supplementation with *L. reuteri* LTH2584 mitigates weight gain during risperidone treatment

Based on previous studies on Lactobacillaceae<sup>38</sup> and the metagenomics data above, we hypothesized that these strains may be key constituents in the gut with the potential to stabilize an anti-obesogenic microbiota. Because *L. reuteri* is known to be present in the human gut<sup>39</sup> and is found in food sources such as sourdough bread,<sup>40</sup> we decided to test whether *L. reuteri* could prevent weight gain in the presence of risperidone. Further, because *L. reuteri* is known to produce several biologically active metabolites, we

chose strain LTH2584, which has been sequenced, has a genetic system and can produce reutericyclin.<sup>17,18</sup>

We administered  $3 \times 10^8$  CFUs (100  $\mu$ L) of *L. reuteri* LTH2584 via gavage or vehicle control (PBS) daily over two months to C57BL/6J female mice and assessed the efficacy of those bacteria to mitigate weight gain associated with risperidone treatment (*ad libitum* in drinking water) under a standard chow (2920X) diet. Four cohorts of 10 mice were treated for 63 days: 1) PBS, 2) risperidone, 3) LTH2584 cells, and 4) LTH2584 cells plus risperidone (Figure 2). At the endpoint, animals treated with



buffer gained  $4.41 \pm 0.42$  g and represents standard growth of C57BL/6J female mice under the conditions of our experiment. In contrast, animals treated with risperidone gained an average of  $11.42 \pm 0.72$  g ( $\Delta = 7.01$  g), while animals receiving LTH2584 cells gained  $4.24 \pm 1.21$  g. Mice treated with both LTH2584 cells and risperidone gained  $7.34 \pm 0.5$  g ( $\Delta = 2.93$  g), significantly less than risperidone treated animals ( $p = 0.0007$ ). The relative reduction is 58%, indicating that LTH2584 cells can mitigate risperidone-induced weight gain in mice. This trend was also observed upon dissection of the visceral fat (Figure 2(c)). The ratio of visceral fat mass to total mass for each animal demonstrated that the deflection in weight gain is due to a reduction of fat (Figure 2(d)).

### Synthetic reutericyclin is sufficient to prevent risperidone-induced weight gain

Because *L. reuteri* LTH2584 is known to affect microbial communities *in vitro*,<sup>41,42</sup> we sought to investigate if reutericyclin alone was sufficient to mitigate weight gain as observed above. To answer this, we synthesized (S)-reutericyclin using L-leucine as a precursor molecule (see Supplemental Methods) and tested its ability to prevent RIWG. C57BL/6J female mice were treated with reutericyclin via gavage (2.5 µg/day), risperidone (20 µg/mL, *ad libitum*), reutericyclin plus risperidone, or with buffer (Figure 3). Risperidone and control animals received 100 µL of 2.5% DMSO in PBS daily as the vehicle control for reutericyclin treatment. After 25 days, risperidone-treated animals gained  $3.58 \pm 0.38$  g, whereas animals treated with reutericyclin and risperidone gained  $2.5 \pm 0.43$  g, a statistically significant reduction in weight gain (2-way ANOVA,  $*p = 0.039$ ) (Figure 3).

There was no statistically significant difference in weight gain between cohorts receiving reutericyclin and buffer control indicating that reutericyclin alone does not lead to weight loss under the conditions of our assay but does prevent weight gain in the presence of risperidone. Further, we synthesized and tested (R)-reutericyclin, by using D-leucine as a precursor molecule, (see Supplemental Methods) which was also capable of deflecting risperidone-induced weight gain (Figure S1), albeit to a lesser extent than (S)-reutericyclin (Figure 3).

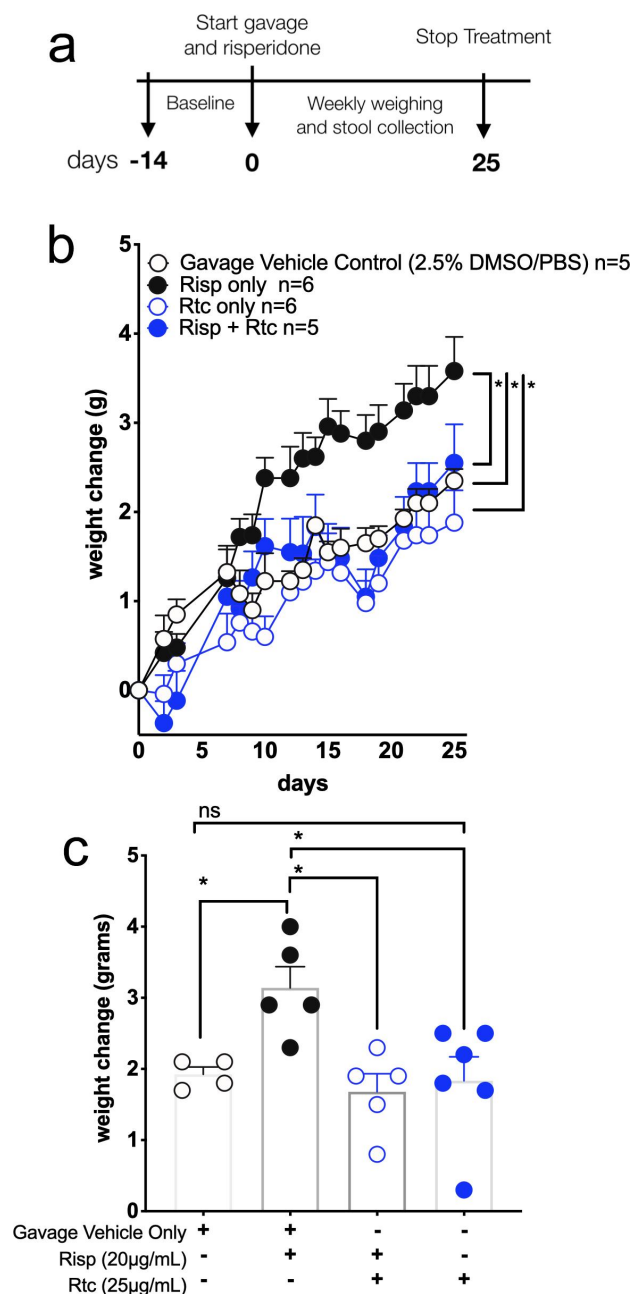


**Figure 3.** Synthetic reutericyclin (Rtc) is sufficient to prevent risperidone-induced weight gain in mice. A) Experimental timeline. Cohorts of 5 mice were allowed to acclimate for two weeks to establish a baseline. Mice were treated with either water or risperidone provided *ad libitum* (20 µg/mL) and gavaged with Rtc (25 µg/mL) in 100 µL PBS with 2.5% DMSO or vehicle, daily. B-C) Rtc mitigates risperidone induced weight gain. During 25 days of treatment, risperidone treated animals (black filled) gained significantly more weight than gavage vehicle control animals (black open), Rtc only (blue open), or Rtc+risperidone treated animals (blue filled) by 2-way ANOVA (B) and Mann-Whitney (C) ( $p < 0.05$ ).



### ***A reutericyclin biosynthesis mutant, LTH2584 $\Delta$ rtcN, does not mitigate risperidone-induced weight gain***

While reutericyclin alone was sufficient to deflect weight gain in the presence of risperidone, we wanted to determine if reutericyclin production by *L. reuteri* was the factor required for prevention of weight gain by LTH2584 cells as shown above. Thus, we created and tested a mutant strain LTH2584  $\Delta$ rtcN, lacking the central biosynthetic gene encoding condensation, adenylation, and thiolation domains demonstrated to be required for reutericyclin production.<sup>17</sup>

We conducted an experiment with 8 cohorts of 7 animals that received 1) vehicle control, 2) risperidone, 3) *L. reuteri* LTH2584 cells, 4) LTH2584 plus risperidone, 5) *L. reuteri* LTH2584  $\Delta$ rtcN, 6) LTH2584  $\Delta$ rtcN plus risperidone, 7) LTH2584  $\Delta$ rtcN plus reutericyclin, and 8) LTH2584  $\Delta$ rtcN plus reutericyclin and risperidone (Figure 4). All 8 cohorts received treatment or vehicle containing

2.5% DMSO daily via gavage. The results indicate that treatment with LTH2584  $\Delta$ rtcN cells alone did not reduce or prevent weight gain compared to the reutericyclin producing strain. Abrogation of weight gain was observed upon simultaneous addition of synthetic reutericyclin alone or in combination with the  $\Delta$ rtcN mutant. Statistical analyses (ANOVA, interaction  $*p < 0.05$ ) indicate that RIWG is mitigated significantly by either LTH2584 or reutericyclin alone but not by the  $\Delta$ rtcN mutant cells alone. There were no statistically significant changes in weight gain for all cohorts where risperidone was not added.

### ***Treatment with *L. reuteri* LTH2584 or synthetic reutericyclin restores energy efficiency without altering food consumption or digestive efficiency***

Because treatment with LTH2584 or with reutericyclin alone did not fully prevent weight gain in the presence of risperidone, we wished to address

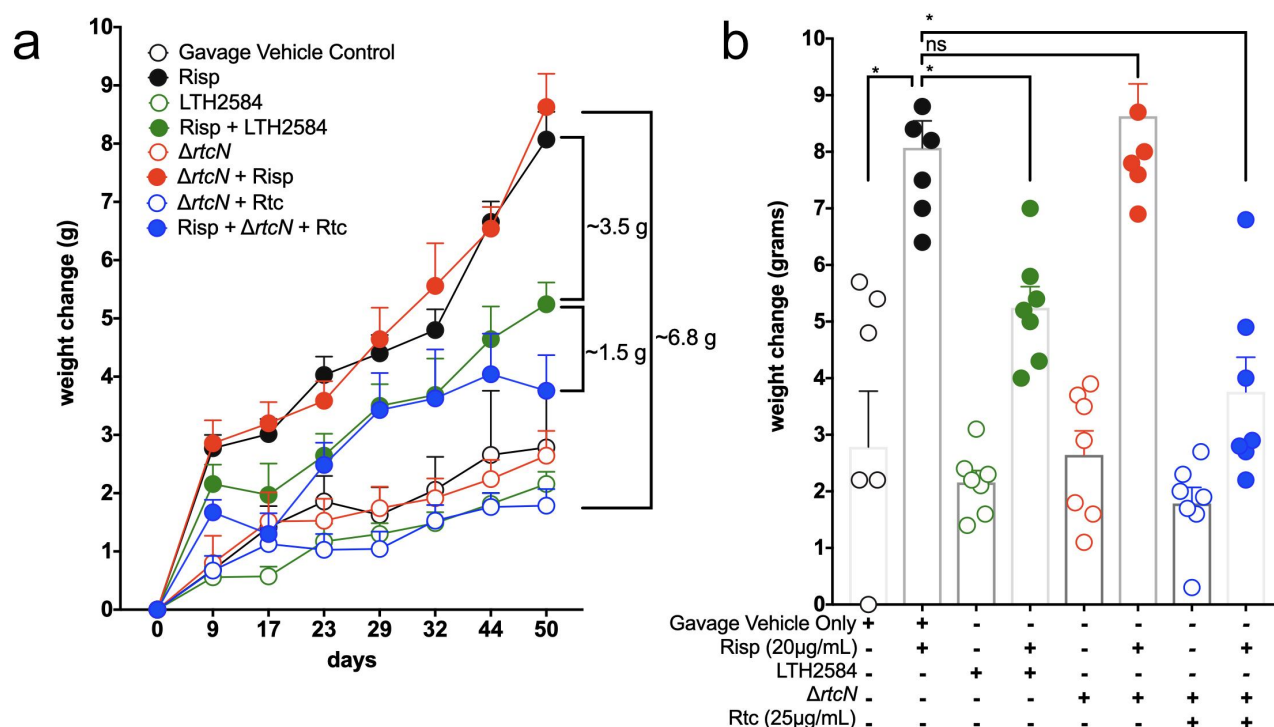


**Figure 4.** Rtc production is required by LTH2584 to mitigate risperidone induced weight gain. Cohorts of 7 mice/group were treated with either the wild-type LTH2584 or LTH2584 $\Delta$ rtcN at  $3 \times 10^8$  CFUs/day with and without risperidone. A cohort of mice were also provided LTH2584 $\Delta$ rtcN + Rtc (25μg/mL). After 50 days of treatment, mice were subjected to metabolic cages to examine feeding and drinking behavior, which we coupled to bomb calorimetry. A-B) LTH2584 $\Delta$ rtcN does not mitigate risperidone induced weight gain. During the 50 days of treatment, risperidone treated animals (black filled) gained significantly more weight than gavage vehicle control animals (black open), LTH2584 treated animals (green open), LTH2584 $\Delta$ rtcN treated animals (red open), and LTH2584 $\Delta$ rtcN + Rtc animals (blue open) by 2-way ANOVA (A) and Mann-Whitney (C) ( $p < 0.05$ ). Importantly, risperidone treated animals (black filled) gained significantly more weight than the Risp+LTH2584 (green filled) and the Risp+  $\Delta$ rtcN+Rtc (blue filled) animals. However, Risp+  $\Delta$ rtcN treated animals (red filled) were not significantly leaner than Risperidone treatment alone.

whether the observed differences might be due to alterations in eating behavior or digestive efficiency. To address this, we performed metabolic caging to quantify food and water intake as well as stool and urine output. We also performed bomb calorimetry to quantify calorie extraction from food (see Methods), as described previously.<sup>35</sup>

After 50 days of treatment, we placed individual animals in metabolic cages for four days and observed that there was no difference in the food intake (Figure 5(a)) or water consumption (Figure 5(b)) per day (pairwise Mann-Whitney,  $p > 0.05$ ). We then assessed feeding efficiency, defined as the change in body mass per gram of food ingested over the 4-day period (Figure 5(c)). Differences are normalized to reflect percentage. Risperidone treated animals gained an average of

50 mg of bodyweight per gram of food ingested relative to 20 mg of bodyweight per gram of food gained by vehicle control animals (Mann-Whitney,  $*p < 0.05$ ). Treatment with either *L. reuteri* LTH2584 cells or synthetic reutericyclin (with or without risperidone) resulted in feeding efficiency similar to vehicle controls. In contrast, animals receiving both risperidone and LTH2584  $\Delta rtcN$  displayed feeding efficiency similar to risperidone treatment alone. Lastly, animals receiving LTH2584  $\Delta rtcN$ , synthetic reutericyclin and risperidone displayed a feeding efficiency similar to vehicle controls, significantly reduced relative to risperidone treatment alone ( $*p < 0.05$ ).

Because feeding efficiency could be affected by caloric extraction from food and/or caloric excretion in stool, we subsequently performed bomb

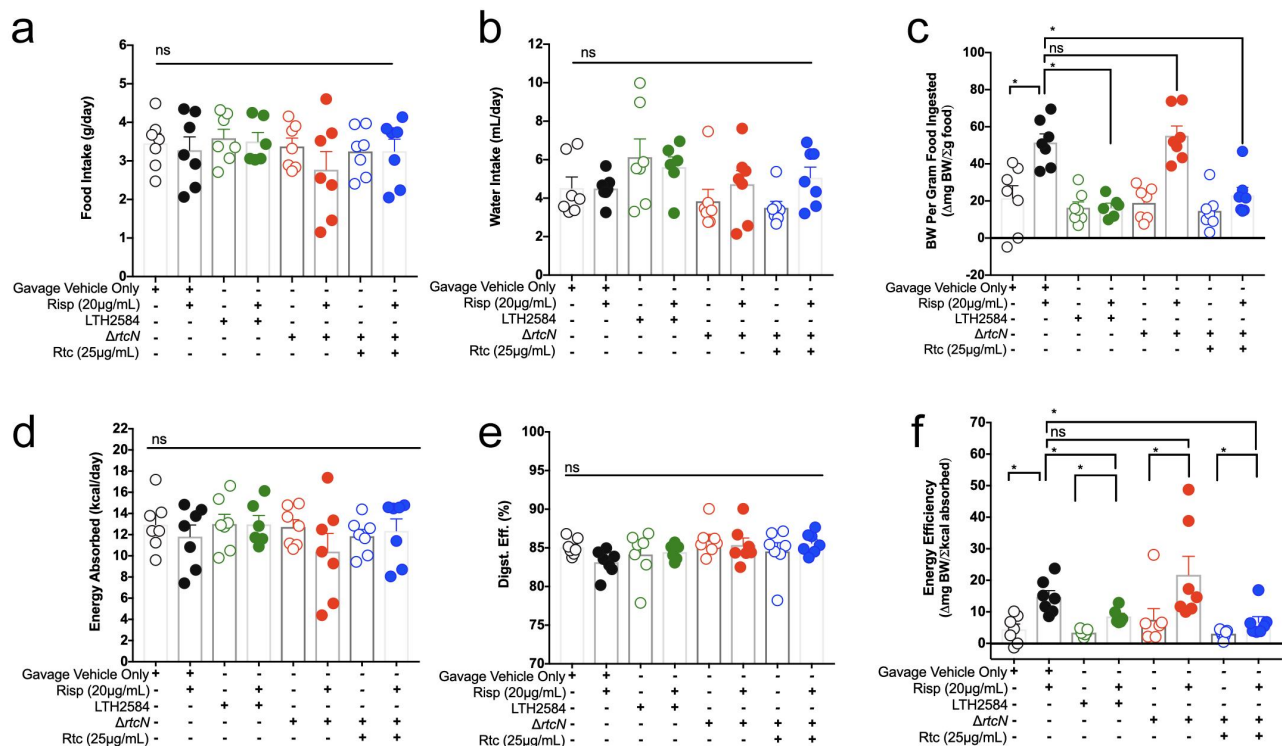


**Figure 5.** Rtc production by LTH2584 restores energy efficiency. A-C) Metabolic caging and D-F) bomb calorimetry demonstrates no differences in food intake, water intake, or digestive efficiency, but major differences in weight gain occur per calorie ingested. Animals were placed in metabolic cages for three days, and their average food intake and water intake was calculated. No significant differences were found in the average daily food intake (A) or water intake (B) between any cohort by pairwise Mann-Whitney (ns,  $p > 0.05$ ). C) Body mass gains per gram of food ingested (feeding efficiency,  $\Delta$ mg body mass / total g food ingested) demonstrates that risperidone treated animals (black filled) and Risp+  $\Delta rtcN$  (red filled) gain significantly more weight per gram of food ingested which is corrected by LTH2584 (green filled) or rescue with Rtc (blue filled) (pairwise Mann-Whitney,  $p < 0.05$ ). D) Bomb calorimetry of the stool and food demonstrated no difference in the energy absorbed by each animal or the E) Digestive efficiency of each animal (% of calories from food absorbed) (Mann-Whitney,  $p > 0.05$ ). F) Calculations of energy efficiency ( $\Delta$ mg body mass / total kcal absorbed) demonstrate that risperidone treated animals (black filled) and Risp+ $\Delta rtcN$  (red filled) convert the energy absorbed into significantly more body mass compared to all other groups (pairwise Mann-Whitney,  $p < 0.05$ ).

calorimetry on both food and stool samples to determine the energy absorbed by each animal during the 4-day caging period. These data allow us to calculate digestive efficiency and energy efficiency, as described previously.<sup>35</sup> No differences were found in the energy absorbed (Figure 5(d)) or the percentage of calories extracted from food and lost to stool (digestive efficiency; Figure 5(e)) across cohorts ( $p > 0.05$ ). Digestive efficiency was ~85% for all animals in this study, regardless of treatment.

Similar to feeding efficiency (Figure 5(c)), energy efficiency (Figure 5(f)), is the change in body mass resulting from calories absorbed. Energy efficiency was significantly higher for animals treated with risperidone only or for animals treated with risperidone and LTH2584  $\Delta rtcN$  relative to all other groups (Mann-Whitney,  $*p < 0.05$ ). Treatment with either LTH2584 or synthetic reutericyclin restore energy efficiency for animals receiving risperidone. Thus, prevention of weight gain provided by either reutericyclin or *L. reuteri* LTH2584 is attributable to its effect on energy efficiency.

#### **Both *L. reuteri* LTH2584 and reutericyclin generate distinct shifts in the gut microbiome**

Previous work from our laboratory led us to conclude that gut microbiota constitutes a thermogenic biomass;<sup>43</sup> gut bacteria consume calories thereby contributing to energy balance and subsequent availability of calories for the host. In addition, surgical removal of mouse ceca (~1% body mass) contributed substantially to an overall decrease in energy expenditure (~8% of metabolic rate). Further, we demonstrated that fecal material transplantation was sufficient to mitigate weight gain in the presence of risperidone.<sup>14</sup> Together, the results above (Figure 5) and our previous analyses suggest that reutericyclin may elicit its effect via shifts in the microbiota.

We performed microbiome profiling from cohorts tested in this study (Figures 2–4). For each experiment we extracted DNA from stool or cecum, performed 16S sequencing, and analyzed the data using the QIIME2 platform.<sup>32</sup> We examined shifts associated with treatments by LTH2584 cells (Figures 6 (stool) and 8 (cecum)) or synthetic

(S)-reutericyclin (Figures 7 (stool) and 9 (cecum)). For each treatment group, beta diversity was assessed and presented using a representative principal coordinate analysis (PCoA). Important discriminant features were assessed using random forest (with Boruta) and statistically by linear discriminant analysis with effect size (LEfSe).<sup>30</sup> We found that each treatment group comprised statistically significant changes in the microbiome relative to controls for both stool and cecal contents (Tables 1–8).

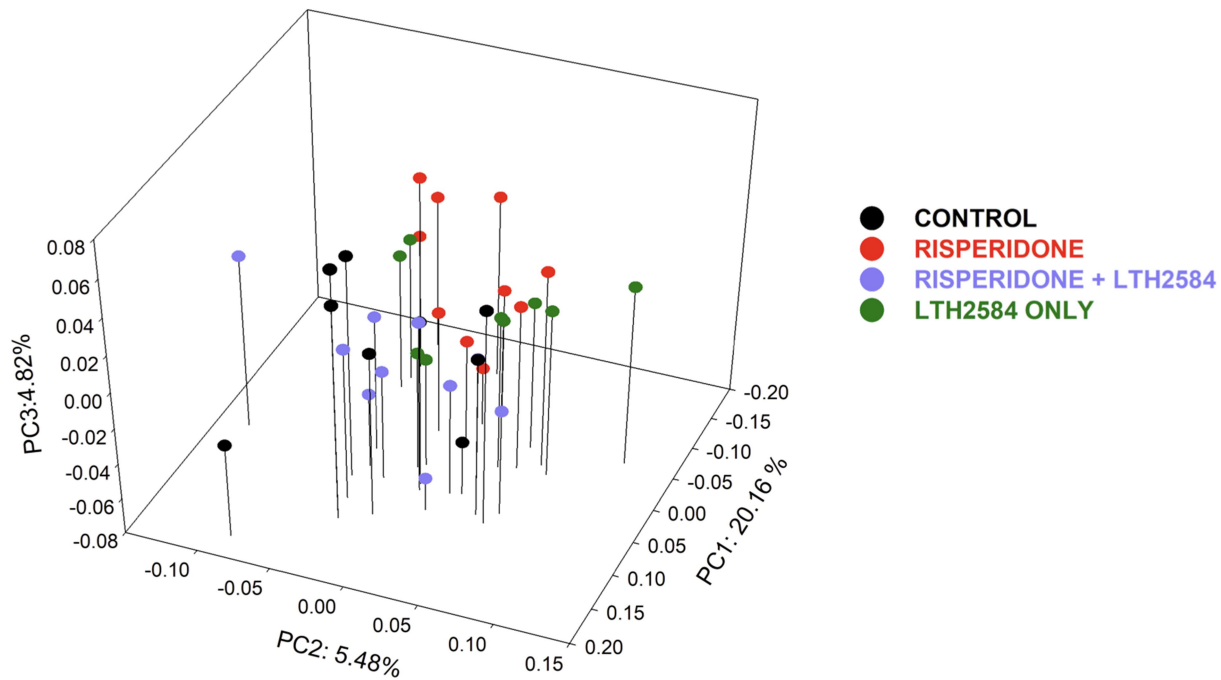
LTH2584 treated animals had stool samples (Figure 6; Table S5) that were enriched with *Adlercreutzia*, *Akkermansia*, and *Angelakisella*, and others (Figure 6(c)). (S)-Reutericyclin treated animals had stool samples (Figure 7; Table S6) that were enriched with *Colidextribacter*, *Lachnospiraceae*, and *Ruminococcaceae* (Figure 7(c)). Similarly, LTH2584 treated animals had cecal samples (Figure 8; Table S7) that were enriched with several members of the *Lachnospiraceae*, and *Ruminococcaceae* and (S)-Reutericyclin treated animals had cecal samples (Figure 9; Table S8) that were enriched with *Lachnospiraceae* family members.

The data indicate that each treatment group is characterized by distinct bacterial taxa although reutericyclin appears to have altered the microbiota to a lesser extent than did LTH2584, at least by 16S analysis. Overall, synthetic reutericyclin and LTH2584 appear to support communities including the *Ruminococcaceae* and *Lachnospiraceae*, known butyrate producers. Lastly, because LTH2584 and reutericyclin treatment in conjunction with risperidone resulted in unique microbiomes relative to control animals, the prevention of weight gain is not due to a return to a control state but instead corresponds to a new anti-obesogenic microbiota.

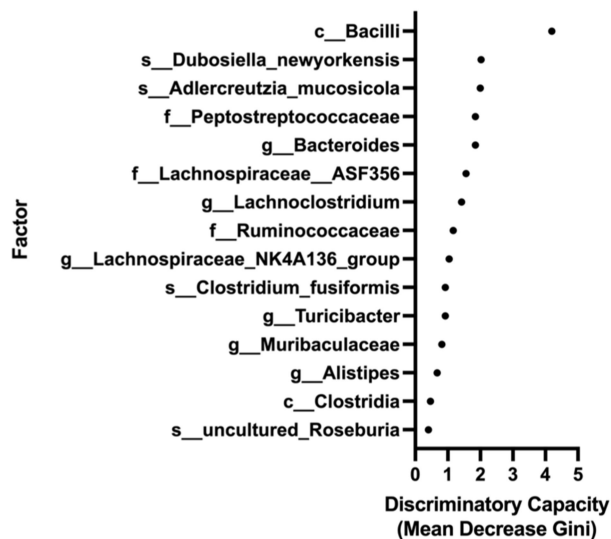
#### **Machine learning and ridge regression identifies factors to predict weight gain in animals supplemented with *L. reuteri* or reutericyclin**

Both LTH2584 and synthetic reutericyclin prevented weight gain in the presence of risperidone and both produced similar shifts in resulting microbiota. Thus, we sought to identify additional factors that might define obesogenic or anti-obesogenic states. We took a machine learning approach to identify discriminators within the

a



b



c

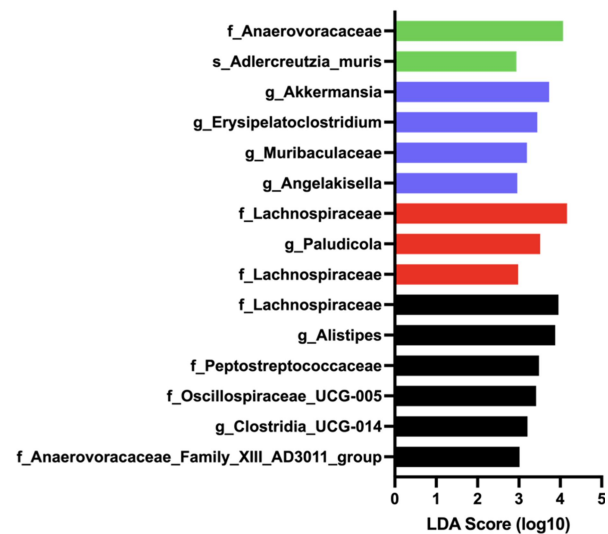


**Figure 6.** *L. reuteri* LTH2584 generates distinct shifts in stool microbiome relative to risperidone treatment or vehicle control. A) Principal Coordinate Analysis following Weighted Unifrac for 16S sequencing of stool from animals treated with vehicle (black), risperidone (red), LTH2584 (green) or both risperidone and LTH2584 (purple). B) Random forest (with Boruta) analysis of discriminatory features for the dataset in A. C) LEfSe analysis of discriminatory features for the dataset in A.

microbiome that are associated with induction of weight gain by risperidone or mitigation of weight gain by LTH2584 or reutericyclin (Figure 10).

We conducted shotgun metagenomics on stool from cohorts in Figures 2–4 as described in

Methods (NovaSeq 2 × 150PE, >10 million reads per sample). We then implemented random forest (with Boruta) to identify the discriminant metagenomes capable of distinguishing between treatment groups (Figures 10(a,d)). The capacity for



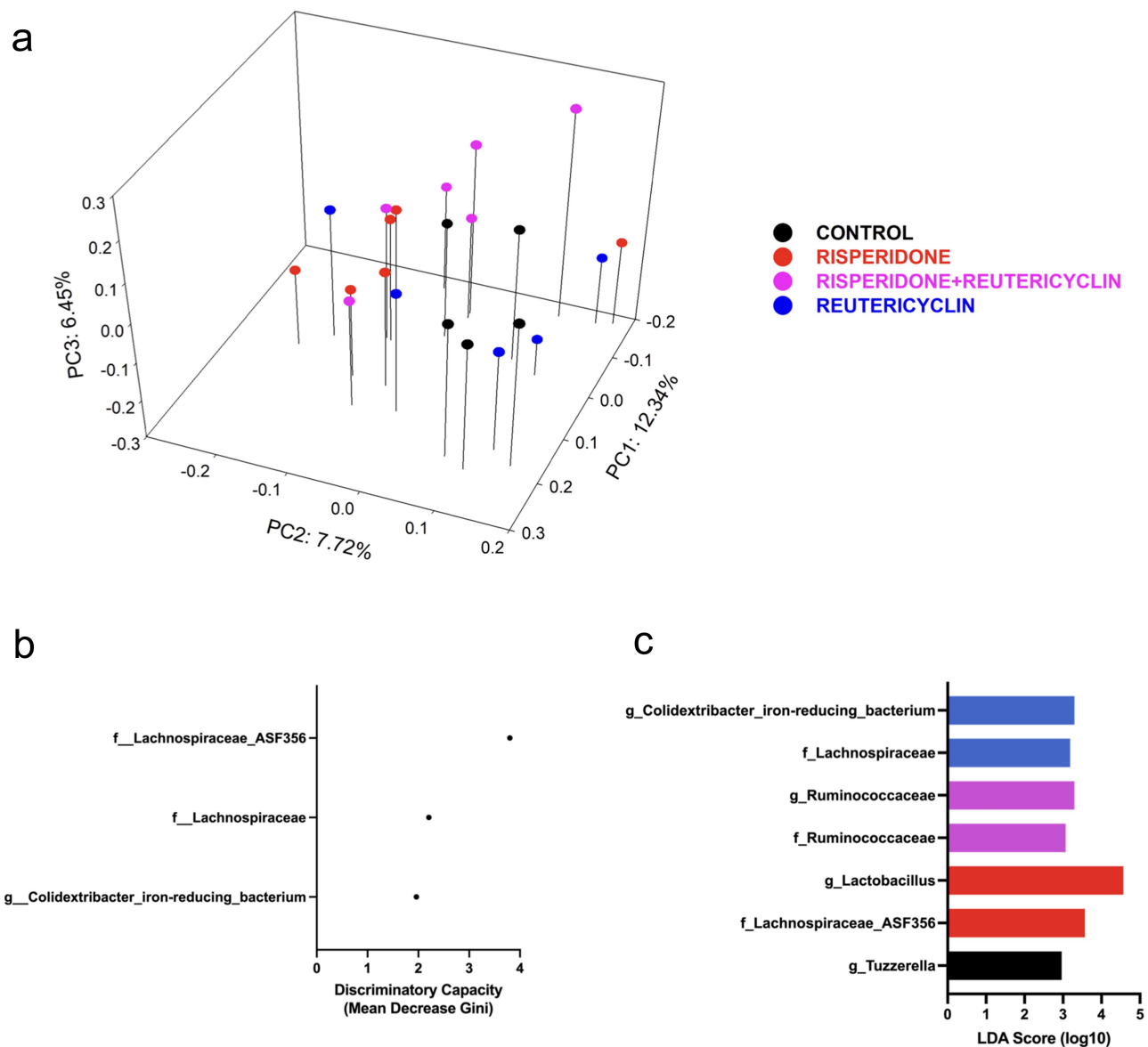


**Figure 7.** Reutericyclin generates distinct shifts in stool microbiome relative to risperidone treatment or vehicle control. A) Principal Coordinate Analysis following Bray-Curtis for 16S sequencing of stool from animals treated with vehicle (black), risperidone (red), reutericyclin (blue) or both risperidone and reutericyclin (pink). B) Random forest (with Boruta) analysis of discriminatory features for the dataset in A. C) LEfSe analysis of discriminatory features for the dataset in A.

**Table 1.** Permuted multivariate analysis of variance (PERMANOVA) using ADONIS and dispersion (PERMDISP) analyses of LTH2584 study using stool samples.

DIVERSITY METRIC		PERMANOVA	PERMDISP	ADONIS
Unweighted Unifrac	t	1.798848	0.940544	$R^2$ 0.13698
	p-value	<b>0.001</b>	0.451	<b>0.001</b>
Weighted Unifrac	t	8.515259	0.734188	$R^2$ 0.429011
	p-value	<b>0.001</b>	0.494	<b>0.001</b>
Bray Curtis	t	2.834562	2.739339	$R^2$ 0.200069
	p-value	<b>0.001</b>	<b>0.037</b>	<b>0.001</b>
Jaccard	t	1.474026	2.922399	$R^2$ 0.115092
	p-value	<b>0.001</b>	<b>0.036</b>	<b>0.001</b>

Significant  $p$ -values at  $p \leq 0.05$  are highlighted in bold.

**Table 2.** PERMANOVA pairwise results from LTH2584 study using stool samples.

TREATMENT COMPARISON		UNWEIGHTED UNIFRAC	WEIGHTED UNIFRAC	BRAY CURTIS	JACCARD
Control vs. Risperidone	pseudo-F	2.018956	17.24643	3.917098	1.542823
	<i>p</i> -value	<b>0.004</b>	<b>0.001</b>	<b>0.001</b>	<b>0.001</b>
Control vs. LTH	pseudo-F	1.946042	9.581155	3.249257	1.47397
	<i>p</i> -value	<b>0.005</b>	<b>0.002</b>	<b>0.001</b>	<b>0.001</b>
Control vs. LTH + Risperidone	pseudo-F	1.84109	2.327409	1.810563	1.460699
	<i>p</i> -value	<b>0.003</b>	<b>0.041</b>	<b>0.004</b>	<b>0.001</b>
Risperidone vs. LTH	pseudo-F	1.914995	2.66034	1.863607	1.365291
	<i>p</i> -value	<b>0.001</b>	<b>0.053</b>	<b>0.013</b>	<b>0.005</b>
Risperidone vs. LTH + Risperidone	pseudo-F	1.694925	12.09876	3.520695	1.63842
	<i>p</i> -value	<b>0.001</b>	<b>0.001</b>	<b>0.001</b>	<b>0.001</b>
LTH vs. LTH + Risperidone	pseudo-F	1.48742	6.020318	2.513865	1.35035
	<i>p</i> -value	<b>0.001</b>	<b>0.001</b>	<b>0.001</b>	<b>0.002</b>

Significant *p*-values at  $p \leq 0.05$  are highlighted in bold.

**Table 3.** Permuted multivariate analysis of variance (PERMANOVA) using ADONIS and dispersion (PERMDISP) analyses of Reutericyclin study using stool samples.

DIVERSITY METRIC		PERMANOVA	PERMDISP		ADONIS
Unweighted Unifrac	t	1.311868	0.975005	$R^2$	0.192104
	<i>p</i> -value	<b>0.028</b>	<b>0.454</b>		0.128
Weighted Unifrac	t	1.426697	1.796587	$R^2$	0.179416
	<i>p</i> -value	0.131	<b>0.101</b>		<b>0.035</b>
Bray Curtis	t	1.122108	1.122108	$R^2$	0.180293
	<i>p</i> -value	<b>0.009</b>	<b>0.009</b>		<b>0.028</b>
Jaccard	t	1.319688	1.282093	$R^2$	0.157553
	<i>p</i> -value	<b>0.025</b>	<b>0.376</b>		<b>0.011</b>

Significant *p*-values at  $p \leq 0.05$  are highlighted in bold.

**Table 4.** PERMANOVA pairwise results from reutericyclin study using stool samples.

TREATMENT COMPARISON		UNWEIGHTED UNIFRAC	WEIGHTED UNIFRAC	BRAY CURTIS	JACCARD
Control vs. Risperidone	pseudo-F	1.110789	3.200249	1.22423	1.679374
	<i>p</i> -value	0.221	<b>0.039</b>	<b>0.008</b>	<b>0.027</b>
Control vs. Reutericyclin	pseudo-F	1.47402	0.702525	1.078402	1.028406
	<i>p</i> -value	0.167	0.582	0.226	0.381
Control vs. Reutericyclin + Risperidone	pseudo-F	0.998839	3.803393	1.132602	1.851064
	<i>p</i> -value	0.472	<b>0.02</b>	0.076	<b>0.021</b>
Risperidone vs. Reutericyclin	pseudo-F	1.546203	0.840506	1.152494	1.05036
	<i>p</i> -value	0.073	0.555	<b>0.044</b>	0.341
Risperidone vs. Reutericyclin + Risperidone	pseudo-F	1.231956	0.824391	1.112671	1.204123
	<i>p</i> -value	0.058	0.524	0.128	0.152
Reutericyclin vs. Reutericyclin + Risperidone	pseudo-F	1.398681	0.622059	1.030533	1.144089
	<i>p</i> -value	0.121	0.654	0.355	0.241

Significant *p*-values at  $p \leq 0.05$  are highlighted in bolds.

**Table 5.** Permuted multivariate analysis of variance (PERMANOVA) using ADONIS and dispersion (PERMDISP) analyses of LTH2584 study using cecum samples.

DIVERSITY METRIC		PERMANOVA	PERMDISP		ADONIS
Unweighted Unifrac	t	4.130326	1.678542	$R^2$	0.398984
	<i>p</i> -value	<b>0.001</b>	0.106		<b>0.001</b>
Weighted Unifrac	t	13.772466	0.346422	$R^2$	0.662794
	<i>p</i> -value	<b>0.001</b>	0.738		<b>0.001</b>
Bray Curtis	t	4.220023	4.177257	$R^2$	0.361345
	<i>p</i> -value	<b>0.001</b>	<b>0.021</b>		<b>0.001</b>
Jaccard	t	1.921277	3.81157	$R^2$	0.209074
	<i>p</i> -value	<b>0.001</b>	0.129		<b>0.001</b>

Significant *p*-values at  $p \leq 0.05$  are highlighted in bold.

**Table 6.** PERMANOVA pairwise results from LTH2584 study using cecum samples.

TREATMENT COMPARISON		UNWEIGHTED UNIFRAC	WEIGHTED UNIFRAC	BRAY CURTIS	JACCARD
Control vs. Risperidone	pseudo-F	6.056726	2.786461	1.227602	1.180359
	p-value	<b>0.003</b>	<b>0.036</b>	0.107	<b>0.008</b>
Control vs. LTH	pseudo-F	3.819347	20.01491	5.128806	2.103304
	p-value	<b>0.003</b>	<b>0.001</b>	<b>0.001</b>	<b>0.001</b>
Control vs. LTH + Risperidone	pseudo-F	7.01924	26.71869	5.796761	2.293004
	p-value	<b>0.002</b>	<b>0.003</b>	<b>0.001</b>	<b>0.001</b>
Risperidone vs. LTH	pseudo-F	3.469467	15.11002	5.69166	2.271649
	p-value	<b>0.009</b>	<b>0.002</b>	<b>0.001</b>	<b>0.001</b>
Risperidone vs. LTH + Risperidone	pseudo-F	2.629491	17.68906	5.791972	2.254973
	p-value	<b>0.001</b>	<b>0.003</b>	<b>0.002</b>	<b>0.001</b>
LTH vs. LTH + Risperidone	pseudo-F	2.957234	2.448226	1.66471	1.400405
	p-value	<b>0.021</b>	<b>0.024</b>	<b>0.004</b>	<b>0.001</b>

Significant  $p$ -values at  $p \leq 0.05$  are highlighted in bold.

**Table 7.** Permuted multivariate analysis of variance (PERMANOVA) using ADONIS and dispersion (PERMDISP) analyses of Reutericyclin study using cecum samples.

DIVERSITY METRIC		PERMANOVA	PERMDISP		ADONIS
Unweighted Unifrac	t	1.319688	1.554993	$R^2$	0.563284
	p-value	<b>0.025</b>	0.062		<b>0.001</b>
Weighted Unifrac	t	1.426697	0.719951	$R^2$	0.360802
	p-value	0.131	0.377		<b>0.001</b>
Bray Curtis	t	1.319688	0.167001	$R^2$	0.166531
	p-value	<b>0.025</b>	0.913		<b>0.049</b>
Jaccard	t	1.319688	1.829765	$R^2$	0.160617
	p-value	<b>0.025</b>	0.225		<b>0.001</b>

Significant  $p$ -values at  $p \leq 0.05$  are highlighted in bold.

**Table 8.** PERMANOVA pairwise results from reutericyclin study using cecum samples.

TREATMENT COMPARISON		UNWEIGHTED UNIFRAC	WEIGHTED UNIFRAC	BRAY CURTIS	JACCARD
Control vs. Risperidone	pseudo-F	1.679374	3.200249	1.22423	1.679374
	p-value	<b>0.027</b>	<b>0.039</b>	<b>0.008</b>	<b>0.027</b>
Control vs. Reutericyclin	pseudo-F	1.028406	0.702525	1.078402	1.028406
	p-value	0.381	0.582	0.226	0.381
Control vs. Reutericyclin + Risperidone	pseudo-F	1.851064	3.803393	1.132602	1.851064
	p-value	<b>0.021</b>	<b>0.02</b>	0.076	<b>0.021</b>
Risperidone vs. Reutericyclin	pseudo-F	1.05036	0.840506	1.152494	1.05036
	p-value	0.341	0.555	<b>0.044</b>	0.341
Risperidone vs. Reutericyclin + Risperidone	pseudo-F	1.204123	0.824391	1.112671	1.204123
	p-value	0.152	0.524	0.128	0.152
Reutericyclin vs. Reutericyclin + Risperidone	pseudo-F	1.144089	0.622059	1.030533	1.144089
	p-value	0.241	0.654	0.355	0.241

Significant  $p$ -values at  $p \leq 0.05$  are highlighted in bold.

each genome to distinguish those groups was plotted as mean decrease Gini score where a higher score correlates with greater discriminatory power. To visualize the association of each metagenome and its impact on weight gain, we initially applied a Multiple Linear Regression (MLR) model, which was observed to be prone to overfitting due to low sample size compared to a high number of discriminant metagenomes generated from Boruta analysis. To address this, we used the ridge regression analysis (Figures 10(b,e)) to constrain the magnitude and plotted resulting

coefficients (Figures 10(c,f)). Collectively, this analysis defined the association between specific metagenomes and weight gain. A MLR model was also used on relative abundance of discriminant bacterial taxa identified from Figures (6(b),7(b)); however, the resulting Spearman's rank correlation indicated a weaker association with weight gain (Adjusted  $r^2 = 0.44$ ,  $p = 0.011$ ) which may be due to low discriminatory and phylogenetic power at species level.<sup>44,45</sup> To improve predictive power of the model, we elected to continue with the ridge regression model. The ridge regression model

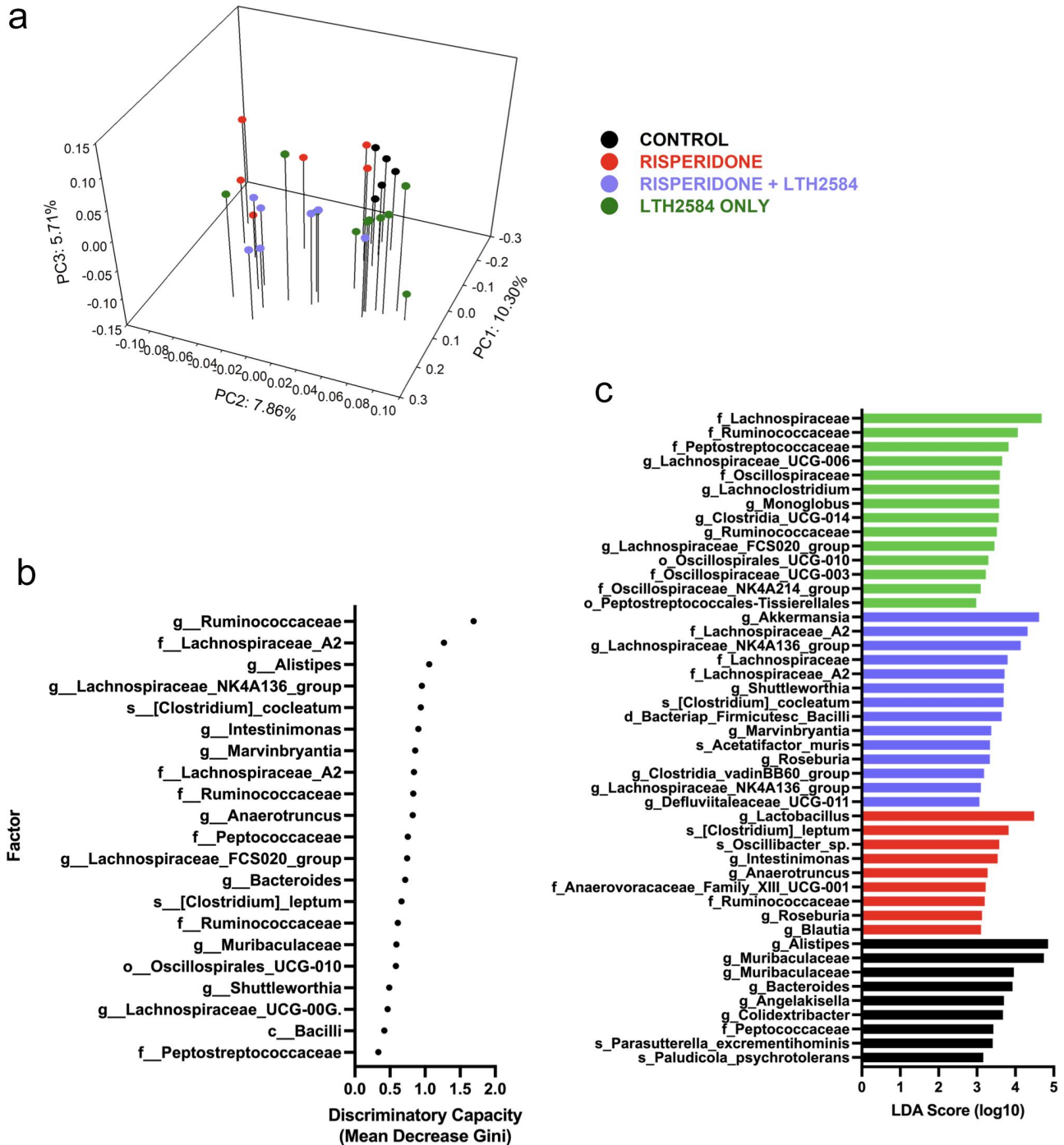


**Figure 8.** LTH2584 generates distinct shifts in the cecal microbiome relative to risperidone treatment or vehicle control. A) Principal Coordinate Analysis following Weighted Unifrac for 16S sequencing of cecal contents from animals treated with vehicle (black), risperidone (red), LTH2584 (green) or both risperidone and LTH2584 (purple). B) Random forest (with Boruta) analysis of discriminatory features for the dataset in A. C) LefSe analysis of discriminatory features for the dataset in A.

using discriminant metagenomes was evaluated by the root mean square error, which measures the average difference between predicted and observed weight values. A low RMSE indicates better predictive accuracy. The model using discriminant

metagenomes and weight gain of mice treated with LTH2584 and risperidone, LTH2584 only, and risperidone only was off by an RMSE value of  $\pm 0.5891$  grams (Figure 10(a)). The model using weight gain of mice treated with risperidone and



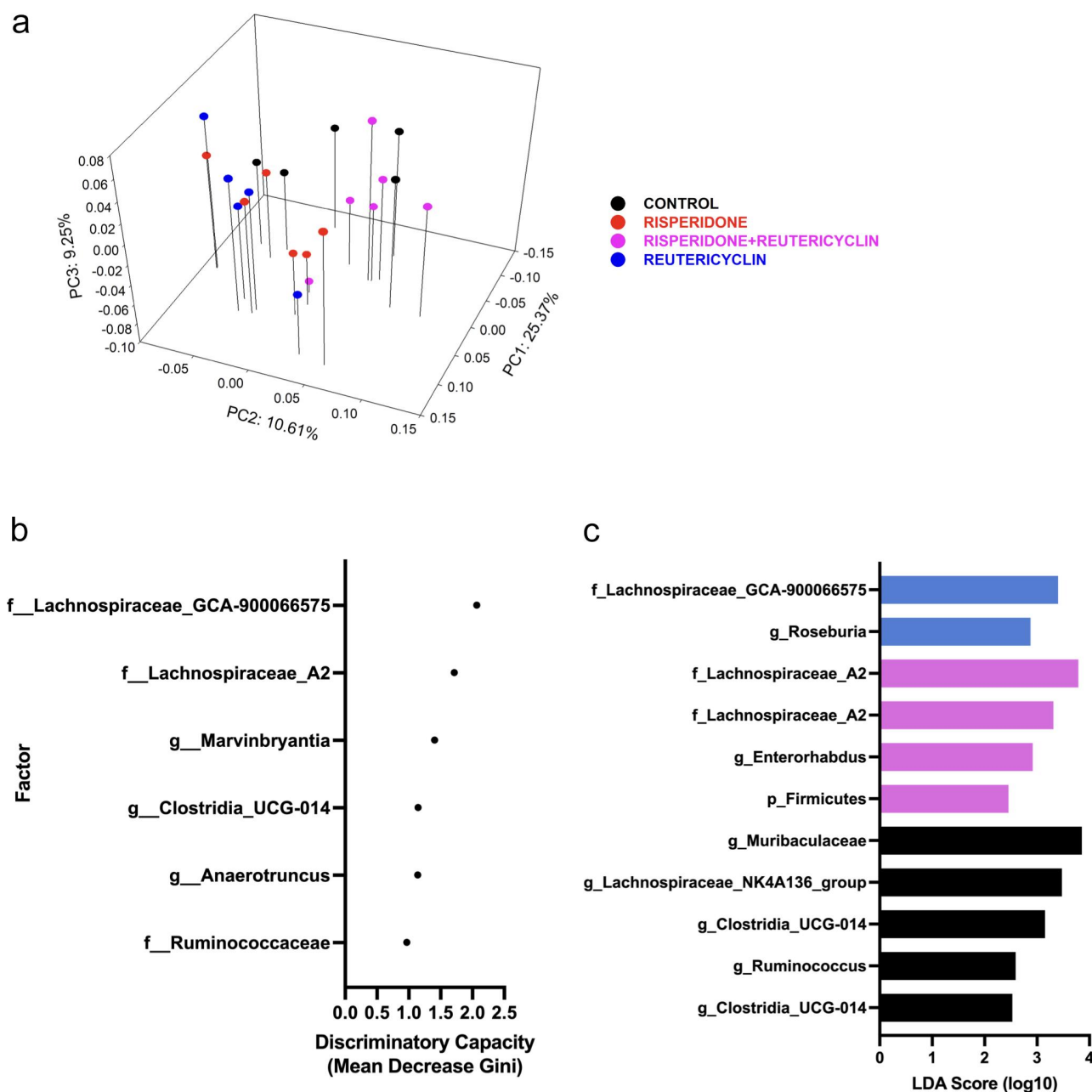


**Figure 9.** Reutericyclin generates distinct shifts in the cecal microbiome relative to risperidone treatment or vehicle control. A) Principal Coordinate Analysis following Weighted Unifrac for 16S sequencing of cecal contents from animals treated with vehicle (black), risperidone (red), reutericyclin (blue), or both risperidone and reutericyclin (pink). B) Random forest (with Boruta) analysis of discriminatory features for the dataset in panel A. C) LefSe analysis of discriminatory features for the dataset in A.

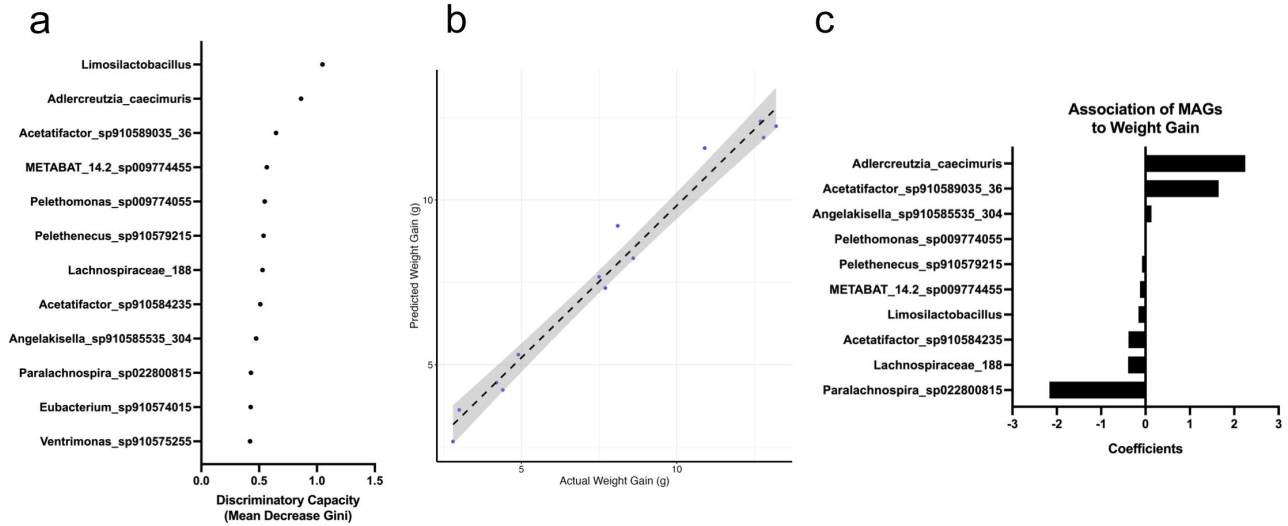
risperidone + reutericyclin was off by an RMSE value of  $\pm 2.913$  grams (Figure 10(b)). Exposure to reutericyclin may not be able to fully parallel complex biological effects caused by LTH2584, which may explain differences in RMSE values between both prediction models, which are still low. Based on the model, the observed and predicted weight gain for both treatments indicates a high capacity for discriminant metagenomes to predict final

weight outcome under the conditions of our experiments.

## Discussion

The microbiome has been associated with the development of metabolic diseases including cardiovascular disease, diabetes, and obesity.<sup>46–50</sup> As a result, development of microbiome-targeted

## LTH2584



## Reutericyclin

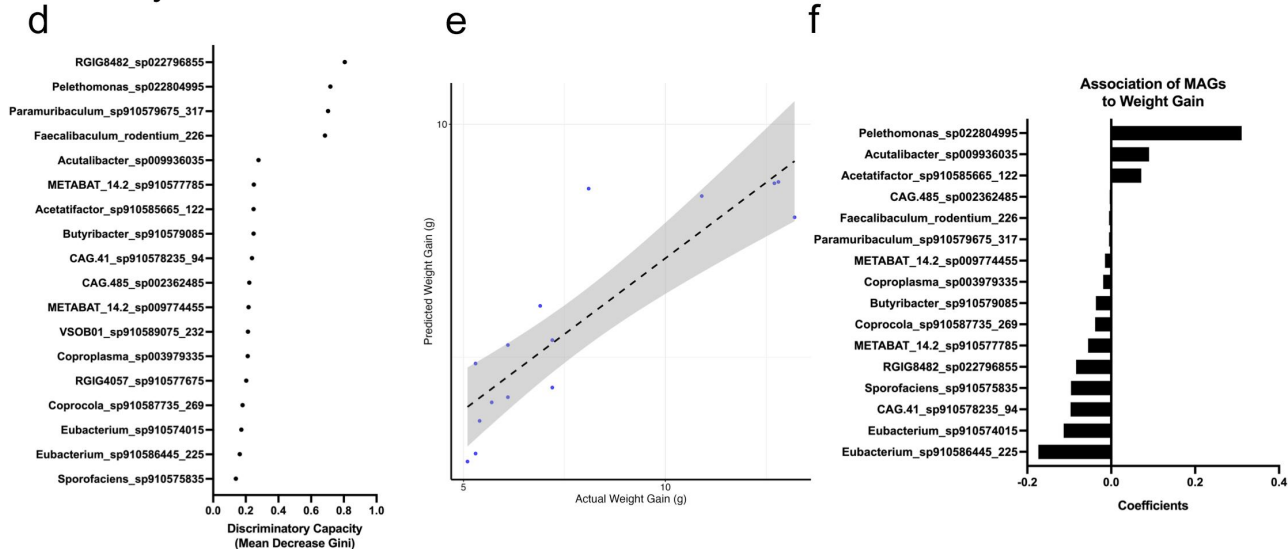


**Figure 10.** Machine learning identifies factors to predict weight gain in animals supplemented with *L. reuteri* or reutericyclin. A and D) A random forest wrapper method, Boruta feature selection algorithm, was applied to coverage of MAGs to reveal discriminatory features from (A) RISP vs. LTH2584+RISP vs. LTH2584 or (D) RISP+RTC vs. RISP from stool (animals in Figures 6 and 7). Random forest was performed on the selected features to generate Gini coefficients. B and E) Ridge regression model trained on MAG coverage of discriminant features to predict weight gain using 10-fold cross validation on samples from animals treated with (B) LTH2584 or (E) reutericyclin. Dashed black line represents perfect fit ( $y=x$ ). Each dot represents one animal. Gray band indicates the 95% confidence interval. C and F) Individual coefficients from Ridge regression model depicting relative importance of discriminant features after L2 regularization. Height of bars indicate magnitude of coefficient for each predictor variable (discriminant feature). Directionality of bars indicates positive or negative association with target variable (weight gain).

therapeutics for specific conditions is highly attractive. In this study, we used a rational approach to identify microbes within lean animals that might prevent risperidone-induced weight gain (RIWG). We identified ~16 metagenomes depleted in the risperidone-treated animals (Figure 1) and chose to focus on *Limosilactobacillus reuteri* as a prime

candidate due to its production of specialized metabolites, known growth requirements, and availability of a genetic system.

We demonstrate that either *L. reuteri* LTH2584 (Figure 2) or synthetic (S)-reutericyclin (Figure 3) are sufficient to mitigate weight gain in the presence of risperidone. We deleted a key component

of the reutericyclin biosynthetic gene cluster, *rtcN*, which eliminated protection from RIWG (Figure 4). Extracellular complementation with synthetic reutericyclin rescued the phenotype, indicating that reutericyclin production by *L. reuteri* is responsible for mitigation of weight gain in the presence of risperidone.

Protection from RIWG by either LTH2584 or synthetic reutericyclin was not due to altered food intake, water intake, energy absorption, or digestive efficiency (Figure 5). However, feeding efficiency and energy efficiency were altered such that risperidone-treated animals gained more weight per gram of food ingested (Figure 5(c)) and gained more weight per kcal ingested (Figure 5(f)). LTH2584 and reutericyclin restored both feeding efficiency and energy efficiency, thereby mitigating RIWG. In contrast, and as expected, the  $\Delta rtcN$  mutant was unable to restore feeding efficiency and energy efficiency. Thus, we conclude that reutericyclin production by LTH2584 is necessary and sufficient for the observed protection to prevent RIWG. Studies using whole-animal calorimetry and microbial supplementation are underway to determine the mechanism of action by which reutericyclin affects energy expenditure.

Because a fecal material transplant from risperidone-treated animals led to statistically significant weight gain in our previous study,<sup>14</sup> we further characterized the microbiome for the cohorts in this study. Changes in gut bacteria using 16S demonstrated that each perturbation resulted in unique features characterizing distinct microbiomes for each treatment group (Figures 6–9). Because three cohorts (controls, synthetic reutericyclin, and *L. reuteri*) did not display enhanced weight gain yet displayed unique microbiomes, we conclude that multiple microbial consortia likely support leanness, as revealed by the Human Microbiome Project.<sup>51</sup> Even in the presence of risperidone, treatment with synthetic reutericyclin or *L. reuteri* generates unique anti-obesogenic or lean promoting microbiota.

While we do not know the mechanism by which reutericyclin mediates protection from risperidone-induced weight gain, we suggest several factors here. *First*, reutericyclin possesses antimicrobial activity and could prevent growth

or expansion of bacteria that contribute to obesity during risperidone treatment. It has been demonstrated that reutericyclin is hydrophobic and can insert into bacterial membranes, thus acting as a proton ionophore to dissipate the membrane gradient and lead to cell lysis.<sup>41</sup> Broadly, it is known that Gram-positive organisms are sensitive to reutericyclin. However, the results from each treatment group including controls (Figures 6–9; Tables S5–8) display significant shifts in members of the Firmicutes (or Bacillota), suggesting that a response to synthetic reutericyclin or *L. reuteri* is strain or consortium dependent.

*Second*, reutericyclin is similar in structure to aryl and acyl homoserine lactones (AHL; Figure S2), which play a role in intercellular bacterial signaling or quorum sensing. Interestingly, an AHL found in *Pseudomonas aeruginosa* was shown to spontaneously convert (at low pH within the mucin barrier) to a tetramic acid which also displays antimicrobial activity; reutericyclin possesses a tetramic acid moiety<sup>42,52</sup> and therefore could play a role in intercellular signaling and thereby promote ecological shifts. This point also raises the possibility that *L. reuteri*, engages in mimicry or competition by using a molecule typically associated with Gram-negative intercellular signaling.

*Third*, reutericyclin could act as a siderophore to mediate iron availability and subsequent changes in microbial composition. It is known that the tetramic acid from *P. aeruginosa* can sequester iron using the same moiety present in reutericyclin. Preliminary data indicate that synthetic reutericyclin can bind iron *in vitro* (Figure S3). Because iron is an essential nutrient and limiting growth factor for many bacteria, alterations in iron availability could have significant impacts on gut microbial structure.<sup>53</sup> All possibilities listed here for reutericyclin activity may function to elicit the results observed in our study.

The major biological question remaining is the mechanism by which microbiota affect weight gain. One hypothesis is that obesogenic microbiota affects nutrient harvest, providing carbon for uptake by the host.<sup>49</sup> A second hypothesis is that microbes in individuals with obesity produce metabolites (e.g. short chain fatty acids) that modulate host metabolism to affect body

mass.<sup>54</sup> A third hypothesis, one that we favor, is that the gut microbiota constitutes a thermogenic biomass such that cecal microbiota in lean animals burn more calories, as suggested previously by our team.<sup>43</sup> In support of this notion, we observe enrichment of fermentation genes in those organisms (Figure S6) contributing most to *prevention* of weight gain as shown in Figure 10(a–c)). In short, a reutericyclin-influenced bacterial consortium may possess enhanced capacity to turnover carbon, thereby preventing calories from being absorbed by the host. Experiments are ongoing to test these possibilities.

## Acknowledgments

The authors gratefully acknowledge the assistance of the Medical College of Wisconsin (MCW) Comprehensive Rodent Metabolic Phenotyping Core and the MCW Biomedical Resource Center for animal work. This research was completed in part with computational resources and technical support provided by the Research Computing Center at MCW. We also thank the University of Wisconsin Biotechnology Center DNA Sequencing Facility for conducting 16S and whole-genome shotgun sequencing.



## Disclosure statement

In accordance with Taylor & Francis policy and my ethical obligation as a researcher, I am reporting that JRK holds U.S. Pat. No. 11,116,748 for use of reutericyclin to prevent weight gain. JRK co-founded Rose Biosciences which holds the exclusive license to said patent. Rose Biosciences may be affected by the research reported in the enclosed paper. JRK has disclosed these interests fully to Taylor & Francis, and JRK has in place an approved plan for managing any potential conflicts arising from that involvement.

## Funding

This work was supported by grants from the NIH (HL134850, DK133121, HL084207 to JLG, A108255 and AG075501 to JRK, HL158900 to TLK, 5F31DK137415 to ABK), and from the Susanna & Justin Mortara Innovation Fund to JRK.

## ORCID

Justin L. Grobe  <http://orcid.org/0000-0001-9737-0873>  
 Tammy L. Kindel  <http://orcid.org/0000-0001-7489-7189>  
 John R. Kirby  <http://orcid.org/0000-0002-2612-0479>

## Author contributions

FA, LK, OD, and JK conceived and designed the experiments. OD conducted mouse experiments. SM grew strains and constructed the *rtcN* mutant. RB and BS synthesized reutericyclin. FA and LK conducted bioinformatic analyses. FA, LK, OD, and JK analyzed the data. JK wrote the manuscript. SK, JG, FS, TK, and VLF contributed to scientific design and editing the manuscript.

## Data availability statement

The authors declare that all supporting data are available within the article and its supplementary files. All DNA sequencing data generated from these studies have been made available in the National Library of Medicine, National Center for Biotechnology Information, Sequence Read Archive as BioProject ID PRJNA859812.

## References

- Donia MS, Cimerancic P, Schulze C, Wieland Brown L, Martin J, Mitreva M, Clardy J, Linington R, Fischbach M. A systematic analysis of biosynthetic gene clusters in the human microbiome reveals a common family of antibiotics. *Cell*. 2014;158(6):1402–1414. doi: [10.1016/j.cell.2014.08.032](https://doi.org/10.1016/j.cell.2014.08.032).
- Zimmermann M, Zimmermann-Kogadeeva M, Wegmann R, Goodman AL. Mapping human microbiome drug metabolism by gut bacteria and their genes. *Nature*. 2019;570(7762):462–467. doi: [10.1038/s41586-019-1291-3](https://doi.org/10.1038/s41586-019-1291-3).
- Blin K, Shaw S, Augustijn HE, Reitz ZL, Biermann F, Alanjary M, Fetter A, Terlouw BR, Metcalf WW, Helfrich EJN, et al. antiSMASH 7.0: new and improved predictions for detection, regulation, chemical structures and visualisation. *Nucleic Acids Res*. 2023;51(W1):W46–W50. doi: [10.1093/nar/gkad344](https://doi.org/10.1093/nar/gkad344).
- Cimerancic P, Medema M, Claesen J, Kurita K, Wieland Brown L, Mavrommatis K, Pati A, Godfrey P, Koehrsen M, Clardy J, et al. Insights into secondary metabolism from a global analysis of prokaryotic biosynthetic gene clusters. *Cell*. 2014;158(2):412–421. doi: [10.1016/j.cell.2014.06.034](https://doi.org/10.1016/j.cell.2014.06.034).
- Donia MS, Fischbach MAHM. Small molecules from the human microbiota. *Science*. 2015;349(6246):1254766. doi: [10.1126/science.1254766](https://doi.org/10.1126/science.1254766).
- Muller S, Strack SN, Ryan SE, Shawgo M, Walling A, Harris S, Chambers C, Boddicker J, Kirby JR. Identification of functions affecting predator-prey interactions between *myxococcus xanthus* and *Bacillus subtilis*. *J Bacteriol*. 2016;198(24):3335–3344. doi: [10.1128/JB.00575-16](https://doi.org/10.1128/JB.00575-16).
- Sharon G, Garg N, Debelius J, Knight R, Dorrestein P, Mazmanian S. Specialized metabolites from the microbiome in health and disease. *Cell Metab*. 2014;20(5):719–730. doi: [10.1016/j.cmet.2014.10.016](https://doi.org/10.1016/j.cmet.2014.10.016).



8. Muller S, DeLeon O, Atkinson SN, Saravia F, Kellogg S, Shank EA, Kirby JR. Thiocillin contributes to the ecological fitness of *Bacillus cereus* ATCC 14579 during interspecies interactions with *myxococcus xanthus*. *Front Microbiol.* **2023**;14:1295262. doi: [10.3389/fmicb.2023.1295262](https://doi.org/10.3389/fmicb.2023.1295262).
9. Andric S, Meyer T, Ongena M. *Bacillus* responses to plant-associated fungal and bacterial communities. *Front Microbiol.* **2020**;11:1350. doi: [10.3389/fmicb.2020.01350](https://doi.org/10.3389/fmicb.2020.01350).
10. Scherlach K, Hertweck C. Chemical mediators at the bacterial-fungal interface. *Annu Rev Microbiol.* **2020**;74(1):267–290. doi: [10.1146/annurev-micro-012420-081224](https://doi.org/10.1146/annurev-micro-012420-081224).
11. Fung TC, Vuong HE, Luna CDG, Pronovost GN, Aleksandrova AA, Riley NG, Vavilina A, McGinn J, Rendon T, Forrest LR, et al. Intestinal serotonin and fluoxetine exposure modulate bacterial colonization in the gut. *Nat Microbiol.* **2019**;4(12):2064–2073. doi: [10.1038/s41564-019-0540-4](https://doi.org/10.1038/s41564-019-0540-4).
12. Chen J, Huang XF, Shao R, Chen C, Deng C. Molecular mechanisms of antipsychotic drug-induced diabetes. *Front Neurosci.* **2017**;11:643. doi: [10.3389/fnins.2017.00643](https://doi.org/10.3389/fnins.2017.00643).
13. Bahr SM, Tyler BC, Wooldridge N, Butcher BD, Burns TL, Teesch LM, Oltman CL, Azcarate-Peril MA, Kirby JR, Calarge CA. Use of the second-generation antipsychotic, risperidone, and secondary weight gain are associated with an altered gut microbiota in children. *Transl Psychiatry.* **2015**;5(10):e652. doi: [10.1038/tp.2015.135](https://doi.org/10.1038/tp.2015.135).
14. Bahr SM, Weidemann BJ, Castro AN, Walsh JW, deLeon O, Burnett CML, Pearson NA, Murry DJ, Grobe JL, Kirby JR. Risperidone-induced weight gain is mediated through shifts in the gut microbiome and suppression of energy expenditure. *EBioMedicine.* **2015**;2(11):1725–1734. doi: [10.1016/j.ebiom.2015.10.018](https://doi.org/10.1016/j.ebiom.2015.10.018).
15. Lin XB, Liu T, Schmaltz R, Ramer-Tait AE, Walter JW, Gänzle MG. Competitiveness of reutericyclin producing and nonproducing *Limosilactobacillus reuteri* in food and intestinal ecosystems: a game of rock, paper, and scissors? *Lett Appl Microbiol.* **2024**;77(2). doi: [10.1093/lambio/ovae007](https://doi.org/10.1093/lambio/ovae007).
16. Wang L, Ren B, Wu S, Song H, Xiong L, Wang F, Shen X. Current research progress, opportunities, and challenges of *limosilactobacillus reuteri*-based probiotic dietary strategies. *Crit Rev Food Sci Nutr.* **2024**;1–21. doi: [10.1080/10408398.2024.2369946](https://doi.org/10.1080/10408398.2024.2369946).
17. Lin XB, Lohans CT, Duar R, Zheng J, Vederas JC, Walter J, Gänzle M. Genetic determinants of reutericyclin biosynthesis in *Lactobacillus reuteri*. *Appl Environ Microbiol.* **2015**;81(6):2032–2041. doi: [10.1128/AEM.03691-14](https://doi.org/10.1128/AEM.03691-14).
18. Ganzle MG, Holtzel A, Walter J, Jung G, Hammes WP. Characterization of reutericyclin produced by *lactobacillus reuteri* LTH2584. *Appl Environ Microbiol.* **2000**;66(10):4325–4333. doi: [10.1128/AEM.66.10.4325-4333.2000](https://doi.org/10.1128/AEM.66.10.4325-4333.2000).
19. Bolger AM, Lohse M, Usadel B. Trimmomatic: a flexible trimmer for illumina sequence data. *Bioinformatics.* **2014**;30(15):2114–2120. doi: [10.1093/bioinformatics/btu170](https://doi.org/10.1093/bioinformatics/btu170).
20. Eren AM, Vineis JH, Morrison HG, Sogin ML, Jordan IK. A filtering method to generate high quality short reads using illumina paired-end technology. *PLOS ONE.* **2013**;8(6):e66643. doi: [10.1371/journal.pone.0066643](https://doi.org/10.1371/journal.pone.0066643).
21. Li D, Liu CM, Luo R, Sadakane K, Lam TW. MEGAHIT: an ultra-fast single-node solution for large and complex metagenomics assembly via succinct de Bruijn graph. *Bioinformatics.* **2015**;31(10):1674–1676. doi: [10.1093/bioinformatics/btv033](https://doi.org/10.1093/bioinformatics/btv033).
22. Li D, Luo R, Liu C-M, Leung C-M, Ting H-F, Sadakane K, Yamashita H, Lam T-W. MEGAHIT v1.0: a fast and scalable metagenome assembler driven by advanced methodologies and community practices. *Methods.* **2016**;102:3–11. doi: [10.1016/j.ymeth.2016.02.020](https://doi.org/10.1016/j.ymeth.2016.02.020).
23. Langmead B, Salzberg SL. Fast gapped-read alignment with bowtie 2. *Nat Methods.* **2012**;9(4):357–359. doi: [10.1038/nmeth.1923](https://doi.org/10.1038/nmeth.1923).
24. Li H, Handsaker B, Wysoker A, Fennell T, Ruan J, Homer N, Marth G, Abecasis G, Durbin R. The sequence Alignment/Map format and SAMtools. *Bioinformatics.* **2009**;25(16):2078–2079. doi: [10.1093/bioinformatics/btp352](https://doi.org/10.1093/bioinformatics/btp352).
25. Eren AM, Esen ÖC, Quince C, Vineis JH, Morrison HG, Sogin ML, Delmont TO. Anvi'o: an advanced analysis and visualization platform for 'omics data. *Peer J.* **2015**;3:e1319. doi: [10.7717/peerj.1319](https://doi.org/10.7717/peerj.1319).
26. Eren AM, Kiefl E, Shaiber A, Veseli I, Miller SE, Schechter MS, Fink I, Pan JN, Yousef M, Fogarty EC, et al. Community-led, integrated, reproducible multi-omics with anvi'o. *Nat Microbiol.* **2021**;6(1):3–6. doi: [10.1038/s41564-020-00834-3](https://doi.org/10.1038/s41564-020-00834-3).
27. Kang DD, Li F, Kirton E, Thomas A, Egan R, An H, Wang Z. MetaBAT 2: an adaptive binning algorithm for robust and efficient genome reconstruction from metagenome assemblies. *Peer J.* **2019**;7:e7359. doi: [10.7717/peerj.7359](https://doi.org/10.7717/peerj.7359).
28. Campbell JH, O'Donoghue P, Campbell AG, Schwientek P, Sczyrba A, Woyke T, Söll D, Podar M. UGA is an additional glycine codon in uncultured SR1 bacteria from the human microbiota. *Proc Natl Acad Sci USA.* **2013**;110(14):5540–5545. doi: [10.1073/pnas.1303090110](https://doi.org/10.1073/pnas.1303090110).
29. Menzel P, Ng KL, Krogh A. Fast and sensitive taxonomic classification for metagenomics with Kaiju. *Nat Commun.* **2016**;7(1):11257. doi: [10.1038/ncomms11257](https://doi.org/10.1038/ncomms11257).
30. Segata N, Izard J, Waldron L, Gevers D, Miropolsky L, Garrett WS, Huttenhower C. Metagenomic biomarker discovery and explanation. *Genome Biol.* **2011**;12(6):R60. doi: [10.1186/gb-2011-12-6-r60](https://doi.org/10.1186/gb-2011-12-6-r60).
31. Altschul SF, Gish W, Miller W, Myers EW, Lipman DJ. Basic local alignment search tool. *J Mol Biol.* **1990**;215(3):403–410. doi: [10.1016/S0022-2836\(05\)80360-2](https://doi.org/10.1016/S0022-2836(05)80360-2).

32. Bolyen E, Rideout JR, Dillon MR, Bokulich NA, Abnet CC, Al-Ghalith GA, Alexander H, Alm EJ, Arumugam M, Asnicar F, et al. Reproducible, interactive, scalable and extensible microbiome data science using QIIME 2. *Nat Biotechnol.* 2019;37(8):852–857. doi: [10.1038/s41587-019-0209-9](https://doi.org/10.1038/s41587-019-0209-9).
33. Kursa MB, Rudnicki WR. Feature selection with the boruta package. *J Stat Softw.* 2010;36(11):1–13. doi: [10.18637/jss.v036.i11](https://doi.org/10.18637/jss.v036.i11).
34. H. Wickham, C. Sievert “ggplot2 : Elegant Graphics for Data Analysis”. 2016 Springer International Publishing Gewerbestrasse 11, Cham, Ch 6330, Switzerland.
35. Reho JJ, Nakagawa P, Mouradian GC, Grobe CC, Saravia FL, Burnett CML, Kwitek AE, Kirby JR, Segar JL, Hodges MR, et al. Methods for the comprehensive in vivo analysis of energy flux, fluid homeostasis, blood pressure, and ventilatory function in rodents. *Front Physiol.* 2022;13:855054. doi: [10.3389/fphys.2022.855054](https://doi.org/10.3389/fphys.2022.855054).
36. Tay JK, Narasimhan B, Hastie T. Elastic net regularization paths for all generalized linear models. *J Stat Softw.* 2023;106(1). doi: [10.18637/jss.v106.i01](https://doi.org/10.18637/jss.v106.i01).
37. Friedman J, Hastie T, Tibshirani R. Regularization paths for generalized linear models via coordinate descent. *J Stat Softw.* 2010;33(1):1–22. doi: [10.18637/jss.v033.i01](https://doi.org/10.18637/jss.v033.i01).
38. Zheng J, Wittouck S, Salvetti E, Franz CMAP, Harris HMB, Mattarelli P, O’Toole PW, Pot B, Vandamme P, Walter J, et al. A taxonomic note on the genus *Lactobacillus*: description of 23 novel genera, emended description of the genus *Lactobacillus* Beijerinck 1901, and union of *Lactobacillaceae* and *Leuconostocaceae*. *Int J Syst Evol Microbiol.* 2020;70(4):2782–2858. doi: [10.1099/ijsem.0.004107](https://doi.org/10.1099/ijsem.0.004107).
39. Li F, Liu J, Maldonado-Gómez MX, Frese SA, Gänzle MG, Walter J. Highly accurate and sensitive absolute quantification of bacterial strains in human fecal samples. *Microbiome.* 2024;12(1):168. doi: [10.1186/s40168-024-01881-2](https://doi.org/10.1186/s40168-024-01881-2).
40. Su MS, Schlicht S, Gänzle MG. Contribution of glutamate decarboxylase in *Lactobacillus reuteri* to acid resistance and persistence in sourdough fermentation. *Microb Cell Fact.* 2011;10 Suppl 1(S1):S8. doi: [10.1186/1475-2859-10-S1-S8](https://doi.org/10.1186/1475-2859-10-S1-S8).
41. Gänzle MG, Vogel RF. Studies on the mode of action of reutericyclin. *Appl Environ Microbiol.* 2003;69(2):1305–1307. doi: [10.1128/AEM.69.2.1305-1307.2003](https://doi.org/10.1128/AEM.69.2.1305-1307.2003).
42. Kaufmann GF, Sartorio R, Lee S-H, Rogers CJ, Meijler MM, Moss JA, Clapham B, Brogan AP, Dickerson TJ, Janda KD. Revisiting quorum sensing: discovery of additional chemical and biological functions for 3-oxo-N-acylhomoserine lactones. *Proc Natl Acad Sci USA.* 2005;102(2):309–314. doi: [10.1073/pnas.0408639102](https://doi.org/10.1073/pnas.0408639102).
43. Riedl RA, Burnett CML, Pearson NA, Reho JJ, Mokadem M, Edwards RA, Kindel TL, Kirby JR, Grobe JL. Gut microbiota represent a Major thermogenic biomass. *Function (Oxf).* 2021;2(3):zqab019. doi: [10.1093/function/zqab019](https://doi.org/10.1093/function/zqab019).
44. Mignard S, Flandrois JP. 16S rRNA sequencing in routine bacterial identification: a 30-month experiment. *J Microbiol Methods.* 2006;67(3):574–581. doi: [10.1016/j.mimet.2006.05.009](https://doi.org/10.1016/j.mimet.2006.05.009).
45. Janda JM, Abbott SL. 16S rRNA gene sequencing for bacterial identification in the diagnostic laboratory: pluses, perils, and pitfalls. *J Clin Microbiol.* 2007;45(9):2761–2764. doi: [10.1128/JCM.01228-07](https://doi.org/10.1128/JCM.01228-07).
46. Goodrich JK, Davenport E, Beaumont M, Jackson M, Knight R, Ober C, Spector T, Bell J, Clark A, Ley R. Genetic determinants of the gut microbiome in UK Twins. *Cell Host & Microbe.* 2016;19(5):731–743. doi: [10.1016/j.chom.2016.04.017](https://doi.org/10.1016/j.chom.2016.04.017).
47. Ley RE, Turnbaugh PJ, Klein S, Gordon JI. Microbial ecology: human gut microbes associated with obesity. *Nature.* 2006;444(7122):1022–1023. doi: [10.1038/4441022a](https://doi.org/10.1038/4441022a).
48. Turnbaugh PJ, Hamady M, Yatsunenkov T, Cantarel BL, Duncan A, Ley RE, Sogin ML, Jones WJ, Roe BA, Affourtit JP, et al. A core gut microbiome in obese and lean twins. *Nature.* 2009;457(7228):480–484. doi: [10.1038/nature07540](https://doi.org/10.1038/nature07540).
49. Turnbaugh PJ, Ley RE, Mahowald MA, Magrini V, Mardis ER, Gordon JI. An obesity-associated gut microbiome with increased capacity for energy harvest. *Nature.* 2006;444(7122):1027–1031. doi: [10.1038/nature05414](https://doi.org/10.1038/nature05414).
50. Le Chatelier E, Nielsen T, Qin J, Prifti E, Hildebrand F, Falony G, Almeida M, Arumugam M, Batto J-M, Kennedy S, et al. Richness of human gut microbiome correlates with metabolic markers. *Nature.* 2013;500(7464):541–546. doi: [10.1038/nature12506](https://doi.org/10.1038/nature12506).
51. Human Microbiome Project C. Structure, function and diversity of the healthy human microbiome. *Nature.* 2012;486:207–214. doi: [10.1038/nature11234](https://doi.org/10.1038/nature11234).
52. Romano AA, Hahn T, Davis N, Lowery CA, Struss AK, Janda KD, Böttger LH, Matzanke BF, Carrano CJ. The Fe(III) and Ga(III) coordination chemistry of 3-(1-hydroxymethylidene) and 3-(1-hydroxydecylidene)-5-(2-hydroxyethyl)pyrrolidine-2,4-dione: novel tetramic acid degradation products of homoserine lactone bacterial quorum sensing molecules. *J Inorg Biochem.* 2012;107(1):96–103. doi: [10.1016/j.jinorgbio.2011.10.009](https://doi.org/10.1016/j.jinorgbio.2011.10.009).
53. Yilmaz B, Li H. Gut microbiota and iron: the crucial actors in health and disease. *Pharmaceuticals (Basel).* 2018;11(4):98. doi: [10.3390/ph11040098](https://doi.org/10.3390/ph11040098).
54. Thaiss CA, Levy M, Grosheva I, Zheng D, Soffer E, Blacher E, Braverman S, Tengeler AC, Barak O, Elazar M, et al. Hyperglycemia drives intestinal barrier dysfunction and risk for enteric infection. *Science.* 2018;359(6382):1376–1383. doi: [10.1126/science.aar3318](https://doi.org/10.1126/science.aar3318).